PREDICTIVE COMBUSTION TRAJECTORY VISUALIZATION MODEL FOR STUDY OF CONVENTIONAL AND ADVANCED DIRECT INJECTION COMPRESSION IGNITION COMBUSTION MODES

by

ALEXANDER HOWARD DeLOACH

JOSHUA A. BITTLE, COMMITTEE CHAIR
MARCUS D. ASHFORD
GARY C. CHENG

A THESIS

Submitted in partial fulfillment of the requirements
for the degree of Master of Science
in the Department of Mechanical Engineering
in the Graduate School of
The University of Alabama

TUSCALOOSA, ALABAMA

2016

ABSTRACT

There are many diagnostic approaches for determine in-cylinder quantities in an internal combustion engine. Of primary importance in this work are equivalence ratio and flame temperature. These parameters can be measured using expensive and highly modified optical engines or calculated using time consuming computational fluid dynamics and chemical kinetic models. These approaches work well in a lab but become less feasible when trying to implement diagnostics for real world on-board consumer use. With the decreasing cost of in-cylinder pressure transducers, the question arises of the whether or not it is feasible to create a diagnostic model based on in-cylinder pressure data and known engine parameter based on existing engine sensors. Using this model, it may be possible to actively modulate engine parameters to change combustion behavior in order to decrease harmful emissions without penalty to efficiency. In this context, combustion behavior (or a trajectory) is meant to describe the local temperatures and equivalence ratios that exist during burning in a direct injection compression ignition engine's combustion chamber. This work builds on earlier attempts to model combustion trajectories on the equivalence ratio – temperature plane (Φ-T plane), as calculated from cylinder pressure. This work uses a 1-D non-vaporizing spray model with assumed radial profile. The proposed model accounts for the change in cylinder pressure throughout the combustion process by using a time step based on the resolution of the cylinder pressure data. Based on the predicted equivalence ratio, local flame temperature, calculated heat release, and amount of fuel burned at each portion (control volume) of the spray, a plot of the combustion trajectory can be developed. The temperature and equivalence ratio at which the fuel burns can be tracked to give a full mass

weighted history of the combustion event with respect to both the ignition conditions and post-mixing heating and cooling on the Φ-T plane. The model was tested over multiple operating conditions including conventional and late timing diesel combustion, with and without EGR, lower and higher injection pressure. The encouraging results obtained from this study suggest engine control strategies could use this simple approach to reduce harmful emissions in the future.

DEDICATION

This thesis work is dedicated to my wife, Jessie, who has been a constant source of support and encouragement during the challenges of graduate school and life. I am truly thankful for having you in my life. This work is also dedicated to my parents, Steve and Michele DeLoach, who have always loved me unconditionally and whose good examples have taught me to work hard for the things that I aspire to achieve.

LIST OF ABBREVIATIONS

aTDC	after Top dead center
BMEP	Break mean effective pressure
bTDC	before Top dead center
EGR	Exhaust gas recirculation
EOI	End of injection
HRR	Heat release rate
LTC	Low temperature combustion
MFB	Mass fraction burned
Phi (Φ)	Equivalence Ratio
SOC	Start of combustion
TDC	Top dead center

ACKNOWLEDGMENTS

I would first like to thank my thesis advisor, Dr. Joshua Bittle at the University of Alabama. The door to Dr. Bittle's office was always open whenever I ran into a trouble spot or had a question about my research or writing. He consistently allowed this paper to be my own work, but steered me in the right the direction whenever he thought I needed it.

I would also like to thank the experts who were involved in the evaluation of this thesis project: Dr. Marcus Ashford and Dr. Gary Cheng. Without their participation and input, the evaluation could not have been successfully conducted.

TABLE OF CONTENTS

LIST OF TABLES

LIST OF FIGURES

INTRODUCTION

As emissions regulations become stricter worldwide, it becomes even more important to be able to manage emissions. This can be accomplished by aftertreatment, which has been implementing heavily in industry already, and by in-cylinder combustion control whereby engine control parameters are modified to accommodate the reduction of oxides of nitrogen and soot emissions. After-treatment refers to operations performed to exhaust gases before they are release to the atmosphere (dealing with emissions that were created in combustion event). These include, but are not limited to, such devices as catalytic converters and diesel particulate filters (DPF). When regulations began to be instituted, after-treatment was sufficient to meet requirements. As these regulations become more strict on all forms of harmful exhaust emissions, the amount of aftertreatment needed becomes obtrusive and uneconomical [1] . In-cylinder combustion controls refer to control strategies that help lower the amount of emissions produced in the first place. One in-cylinder control strategies is the introduction of exhaust gas back into the cylinder (internal or external exhaust gas recirculation) which helps lower combustion temperatures and decreasing NOx emissions, but often increases soot emissions. Other strategies include higher pressure fuel injection and smaller holes in the injector tip. The last two strategies help vaporize fuel leading to a more complete burn and reducing soot constituents. A newer and more complex method of in-cylinder combustion control method used for reducing these emissions in diesel engines is low temperature combustion (LTC). This usage of the LTC method in commercial applications has some barriers, including limited load range, stable operating conditions, and a lack of onboard diagnostics to determine active control

changes during operations. Without on-board emissions diagnostics, it becomes necessary to be able to predict emissions to be used in active control based on engine parameters and some relatively easy to measure engine outputs. Kook [2] has complied a comprehensive comparison on the effects of exhaust gas recirculation (EGR) and LTC in a diesel combustion scenario determining the anticipated differences between combustion predictions for both conventional and LTC modes. These observations include the effect of lowering NOx emissions as EGR rate increases, decreases in soot as temperature increases, and the effect of lower temperatures with later injection timing. Kook was able to plot an idealized path of the combustion trajectories on the equivalence ratio-temperature plane as charge oxygen concentration (EGR) changes. The work presented here synthesizes a combustion trajectory model that could be used for future onboard control tools.

Control strategies and emissions predictions are very active areas for research related to internal combustions engines. A literature review shows significant focuses on both engine simulation and emissions predications models [3-6] and real-time closed loop control methods [7-12]. The work presented here is a proof of concept for a predictive model that could begin to bridge the gap between these two focuses of research, with special consideration for low temperature combustion modes, though some high load conditions are evaluated here.

As stated above, one of the major questions with regards to filling the gap between modeling and control is whether it is feasible to create a model with enough detail without using a full computational fluid dynamics suite. Presently, using a computational fluid dynamics (CFD) model would be impractical for use in an onboard system due to the time associated with running a CFD model. Initial work by Bittle and Jacobs [13] pursued reduced computational time at the cost of complexity, however it suffered from an inability to capture injection pressure

effects. Building on that work, a more advanced spray model developed by Musculus and Kattke [14] was integrated, however the predictions were not able to capture a weighted distribution of burned fuel [15]. The earlier work modified the code of [15] to account for the distribution of burned fuel. The work presented here modifies the code even further to attempt a rudimentary accounting of the locations in the spray likely to be burning by considering the chemical kinetics for changing oxygen concentration. These modifications should give a more accurate indication of the temperature and equivalence ratios which are most dominant during combustion at a given test condition.

Other aspects of the original prediction are based on the models presented and assembled by Gao et al. [5] who created a simplified two-zone model that had the ability to track combustion trajectory throughout the reaction zone (equivalence ratio and reaction temperature) [5]. This model was able to predict the cylinder pressure by using a complex heat release model. This feature, however, is not utilized in the present work since the prediction is based on real time cylinder pressure measurement collected by on-board transducers.

The Musculus and Kattke spray model [14] uses a one-dimensional model to analyze a transient diesel injector jet. This model uses conservation of mass and momentum equations of the fuel as it is being injected in to the system and is calculated at each time step from the beginning of injection up to the end of combustion. The change in mass of fuel in each control volume at the next time step is determined by the net mass flux into each control volume given in the following equation,

$$m_{f,i}^{t+1} = m_{f,i}^{t} + \rho f \left[\left(\beta \overline{\overline{X_f}} f \overline{\overline{u}} A \right)_{i-1}^{t} - \left(\beta \overline{\overline{X_f}} f \overline{\overline{u}} A \right)_{i}^{t} \right] \Delta t \qquad (I)$$

where the superscripts represent the time step counts, subscripts represent the axial control volume index, and Δt is the time step size. $\overline{\overline{X_f}}$ is the cross-sectional average volume ratio between the fuel and the volume of control volume, $A\Delta z$, as related in the following equation,

$$\overline{\overline{X_f}} = \frac{m_f/\rho_f}{A\Delta z} \quad (\text{II})$$

where Δz is the radial width of the control volume. The cross-sectional averaged volume ratio can also be related to the centerline volume ratio, $\overline{X_{f,c}}$, in a one dimensional model by the following equation,

$$\overline{\overline{X_f}} = \frac{\alpha^2}{(\alpha+1)(\alpha+2)}\overline{X_{f,c}} \quad (\text{III})$$

where α is a value that changes for ∞ near the injector tip to 1.5 at some distance downstream to account for the change in shape of the spray. The ratio of the turbulent mean quantities at each radial position to the centerline mean mass can be represented by a Gaussian-like error function in the following equation,

$$\frac{\overline{X_f}}{\overline{X_{f,c}}} = (1-\xi^{\alpha})^2 \quad (\text{IV})$$

where ξ is the ratio of the radial position over the radius of the spray at each axial position, $\frac{r}{R}$. A similar method is also used to calculate the velocity of the fuel in each control volume. The use of this distribution helps describe the velocity profile in a transient and fully developed diesel jet. This model shows agreement with quantitative optical diagnostic techniques [16]. An in-depth discussion of the Musculus and Kattke model can be found in [14].

While the earlier work [15] was able to predict the temperature and equivalence ratio of fuel packets throughout the entire spray, it only recorded how many packets burned at each temperature and equivalence ratio. A modification to the code was made in a later work to keep track of the amount of fuel being burned. This component of the model is retained to allow for a more accurate qualitative emissions discussion.

The inclusion of a relatively high resolution spray and combustion model (1500 cells; 150 axial and 10 radial) represents a significant increase in computational time. Previous work [13] used a much simpler spray model which only required 10 ms to complete a full combustion cycle, however it was not able to capture injection pressure effects. The model presented here requires a greater amount of computational time, approximately 30 minutes, due to the more complex spray model and mass tracking code. The time associated with the new model would be unacceptable for an on-board diagnostic system. Future work should seek to optimize the code to run more efficiently and possibly decrease the complexity of the model while still maintaining the model's ability to capture effects of EGR, rail pressure, and injection timing. Another course of action would be to use an alternate processing option such as a field programmable gate array to do calculations – a task currently being pursued with promising initial results.

MODEL SUMMARY AND MOTIVATION

The following section will give a detailed written description of the model (available in supporting documents) and solution method. The model takes the following inputs:

- Engine speed
- Intake manifold temperature
- Exhaust gas recirculation (EGR) percent
- Rail pressure
- Fuel flow rate
- Injection timing parameters
- Cylinder pressure

Many of the above stated parameters are set using a full authority engine controller that can be modified to enact different operating conditions in the engine. The engine controller used in the validation experiments is described in more detail in a later section. The only values that are not set, or at least known, in the engine controller are the cylinder pressure and the EGR rate. The cylinder pressure is measured using a Kistler 6058A pressure transducer and in described in more detail in a later section. The EGR rate is calculated based on the measured intake and exhaust carbon dioxide concentrations measured using a standard five gas analyzer. In actual on-board consumer applications the EGR rate would have to be estimated; this is something already done by many production engine controllers.

As part of this initial model development, a single data file is created including the input data for all operating conditions to be processed by the code. Once this data file has been created

including the above stated parameters, the model code can begin calculating the predicted combustion trajectory. The first step in the code is to create files in a specified location where figures throughout the routine will be saved for later viewing. The next step for the code is to read the proper values from the data set for specified operating conditions. The code then goes into a series of sub routines were the injection profile is determined based on measured fuel properties. The volume of the cylinder and the surface area of the cylinder based on engine specifications and crank angle are also determined for use in later sub routines. The main routine then computes the heat release rate (HRR) associated with the measured cylinder pressure. The heat release rate calculation utilizes a basic single zone combustion model with a correlation for the ratio of specific heats. A description of this and other approaches is given by Depcik et al. [17]. The gas constant correlation developed by Brunt and Platts [18] is used. The Hohenberg heat transfer coefficient [19] is used in order to calculate wall heat transfer inside the cylinder. The fuel consumption, as mass fraction burned (MFB), is then determine throughout the combustion duration based on the heat released rate and the known heating value of the fuel. This will be used later in the routine to determine the amount of fuel burned in different time steps. The heat release calculations can be halted once all of the injected fuel is consumed to save time. Most of the calculations up to this point in the model code are well established by authors referenced above. The next section of the routine represents the majority of the modifications done which are unique to this thesis.

The next portion of the code is based on a fuel spray behavior model developed by Musculus and Kattke [14]. This model relies on conservation of mass and conservation of momentum of the fuel as it is being injected in to the system and is calculated at each time step from the beginning of injection up to the end of combustion. The Musculus and Kattke [14]

model makes assumptions that include: the jet behaves as a one dimensional jet with a constant spreading angle, no vaporization, and a no slip boundary condition. The modeled spray volume is discretized into axial control volumes in order to account for the transient behavior of the spray throughout the injection and combustion process. By making this accommodation, the effects of the start and end of injections can be captured. The mixing of the fuel as it is injected into the cylinder can be predicted using some of the parameter set points mentioned earlier which include injection pressure, timing and duration. The parameters are changed based on the operating condition being evaluated. This model takes into consideration the effects of measured exhaust oxygen concentration, the known atmospheric oxygen concentration, and the rate of EGR at each operating condition. In this manner, the equivalence ratio values are based on the calculated global oxygen concentration assuming the EGR and fresh air are well mixed. Once these calculations are completed, the model outputs the axial and radial fuel concentration variations from injector tip to the end of the fuel jet. The radial concentration is predicted based on a Gaussian like error function.

Based on the heat release rate calculated from the global cylinder pressure measurement and the local fuel mixing predictions, a combustion model must be developed that will describe where in the spray combustion is actually taking place. In previous work, the fuel being burned (fuel being removed) was evenly distributed across all the control volume where fuel with within the flammability limits. This approach was unable to accurately describe the different flame structure possible during combustion (premixed and diffusion). Another method used in early attempts by the author was to manually change the flame structure in the code based on peak heat release and end of injection. Changing the flame structure would change where fuel was being burned (evenly distributed for premixed flame, from edges for diffusion flame). This

method was coded but not used in the final model due to the difficulties in being able to accurately predict when certain flame structures are present.

In this work the spatial combustion distribution is determined based on reactivity of fuel at the various equivalence ratios. Outside of the predictive model routine, CANTERA (a chemical kinetics solver add-in to MATLAB) was used to determine the effect of equivalence ratio on the heat release rate. Using n-heptane as a surrogate for diesel fuel, the peak heat release rate in a closed system was determine by simulation for a specific equivalence ratio. This value was determined for equivalence ratios between 0.25 and 5 and then normalized (shown in Figure 1) to the maximum value determined which occurred around an equivalence ratio of 1.25. Based on the spray mixing model, this ratio value is applied throughout all the control volumes in the spray based on the local equivalence ratio. This is done using an interpolation routine that multiplies the ratio by the mass of unburned fuel in each control volume to determine the amount of fuel within each control volume that is considered available to be burned in each time step. This will be referred to as "available fuel" for discussion of the model. This method was used in order to try and account for the effect of chemical kinetics throughout the combustion process instead for a performing a full kinetics model for each control volume at each time step. This is an easy way to partially account for kinetics without the computational time needed for a full scale chemical kinetics model. In this manner the rich fuel near the center of the spray is not considered to be burned automatically.

Using the fuel consumption rate calculated early, the amount of fuel burned in each time step can be calculated. There are now two possible values in each control volume for the amount of fuel contributing to heat release; the mass of unburned burned fuel from the spray model or the calculated available fuel. The minimum value of the two is used to insure that an excessive

amount of fuel is not considered to burn. . These values are now the mass of fuel burned in each control volume. The mass of fuel burned is then removed from the mass of fuel unburned. This methodology allows for both the quantity of fuel and equivalence ratio to be tracked. This is all accomplished by modifying the Musculus and Kattke [14] model.

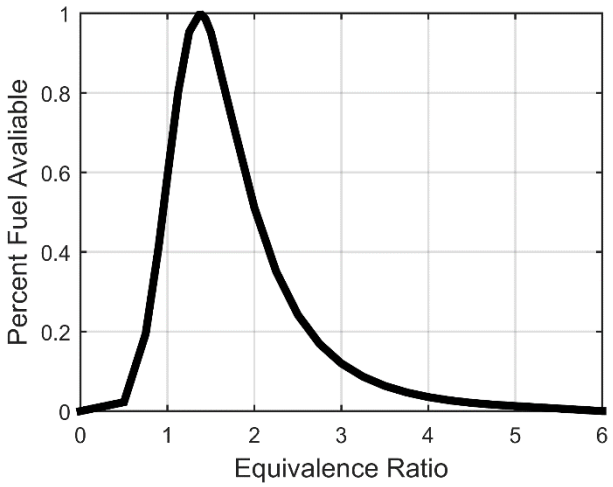

Figure 1 – Percentage of Fuel contributing to Heat Release Rate at heating value

The next step the predictive routine is to calculate the burning temperature for each control volume in a time step. Due to the fast speed at engine operating conditions and the small volume associated with each control volume, the combustion is assumed to occur instantly and adiabatically. Although adiabatic flame temperature can be affected by many things, this model uses simplified calculations affected by EGR, equivalence ratio, and initial temperature. A 2-D look up table is utilized to determine the flame temperature of each control volume. The look up table was generated outside of the model based on a simplified equilibrium solver taking into consideration 13 species and simple reactions using a diesel substitute of $C_{12}H_{23}$ and takes into consideration the effect of EGR and equivalence ratio on the flame temperature. The table was calculated with an initial temperature of 700K but can be compensated for initial temperature differing from 700 K by adding an offset shown in the example below.

$$Tflame(1000\,K) \cong Tflame(700\,K) + 300\,K \quad (V)$$

It was determined that over the 700 to 1000 K initial temperature range with no EGR, there is less than a 4 degree difference between the full adiabatic flame temperature solver and the above stated look up with simplification. As EGR is increased to 50%, the differences increase non-linearly to 12 degrees. This error is assumed negligible in the scope of this model.

The initial temperature can be calculated based on how the temperature increases or decreases during compression, combustion, and expansion. Before combustion begins, the fuel is assumed to be at the bulk gas temperature. Once combustion begins, the unburned fuel increases instantly to the calculated adiabatic flame temperature as stated above. The burned fuel is tracked as it mixes and heats (or cools) based on the bulk gas behavior. The heating (or cooling) will occur based on how the bulk gas temperature changes by the ratio of specific heats as shown below.

$$\Delta T_{burned} = C_{v,burned}/C_{v,bulk} * \Delta T_{bulk} \quad (VI)$$

This states that the specific energy change in the mixture due to the expansion in the cylinder and is the same for both the unburned and burned mixtures. The temperature change can be related to the specific heats at the mixture temperature. The bulk gas temperature can be determined based on the ideal gas law. From this, the temperature change not attributed to combustion can be calculated. This is done for each control volume in the spray.

Once the flame temperature and post combustion mixing temperature for each control volume is determined, 2-D contour plots can be created where the x axis represents the reaction temperature in Kelvin and the y-axis represents the equivalence ratio (Φ). The mass of fuel burned can then be plotted on the Φ-T plane. The "ignition locations" plot represents ignition conditions at which fuel ignited. The "posting mixing heating and cooling" plot represents how

the fuel mixes and heats or cools after the ignition process. The significance of these plots will be discussed in more detail in a later section. During each time step, all the masses of fuel burned at each condition are summed and plotted. These values are tracked from one time step to the next and the new mass is added to the plot as the routine continues. By recording the mass of fuel burned in this manner, the evolution of the combustion process can be seen and by the end of combustion, represents the behavior of the fuel burned throughout the entire process.

The next section highlights some of the important details of the experimental test cell and the remainder of the paper will present the combustion trajectory analysis discussion.

EXPERIMENTAL SETUP FOR ACQUISITION OF VALIDATION DATA

The validation data for the predictive model was taken in previous work done by Bittle [20] using a 4 cylinder medium-duty diesel engine. The engine is equipped with cooled EGR, and a variable geometry turbocharger. The engine is fueled by an electronically controlled high pressure direct injection common rail system. The engine specifications relevant to this study, including nominal engine operating conditions, can be found in Table 1.

Table 1 – Specifications of the medium-duty engine apparatus under investigation.

Bore	106 mm
Stroke	127 mm
Displacement	4.5 L
Rated Power	115 kW at 2400 rev/min
Compression Ratio	16.57 * (nominally 17:1)
Ignition	Compression
Fuel System	Electronic common rail, direct injection
Air System	Variable geometry turbocharger with EGR
Tested Speed	1400,1900,2400 rpm
Tested Load	2 bar BMEP nominal at 1400 rpm, 5.6 bar BMEP at 1900 rpm, 11.3 bar BMEP at 2400 rpm.

* Measured by oil displacement

A nominal load of 2 bar brake mean effective pressure (BMEP) and an operating speed of 1400 revolutions per min (rpm) in all conventional and low temperature combustion comparison conditions. Two other test was performed at 1900 rpm, 5.6 BMEP and 2400 rpm, 11.3 BMEP to represent medium speed, medium load and high speed, high load conditions respectively. The

fuel used for the validation study is commercially-available #2 diesel fuel that was analyzed beforehand. The analyzed fuel properties can be found in Table 2.

Table 2 – Summary of the properties of the fuel used in this study

Property [Standard]	Diesel #2*
Density (kg/m3) [ASTM D4052s]	825.5
Net heat value (MJ/kg) [ASTM D240N]	43.008
Gross heat value(MJ/kg) [ASTM D240G]	45.853
Sulfur (ppm) [ASTM D5453]	5.3
Viscosity (cSt) [ASTM D445 40C]	2.247
Cetane Number [ASTM D613]	51.3
Hydrogen (%-mass) [SAE J1829]	13.41
Carbon (%-mass) [SAE J1829]	85.81
Oxygen (%-mass) [SAE J1829]	0.78
Initial boiling point (°C) [ASTM D1160]	173.4
Final boiling point (°C) [ASTM D1160]	340.5

* Measured or calculated by Southwest Research Institute (San Antonio, Texas)

The experimental results were obtained using the above stated engine managed by a full authority engine controller by NI-Drivven. This setup allowed for control over all enabled electronic systems and the corresponding engine parameters. By manipulating these parameters, multiple operating conditions were obtained for validation.

In-cylinder pressure, which is the basis for most calculations used in comparing engine performance and the driving factor in the predictive model, was measured using a piezo-electric pressure transducer (Kistler 6058A). The pressure transducer was mounded in cylinder #1 (forward most cylinder). The pressure was recorded on a crank angle resolved bases at a 0.2 degree resolution. The in-cylinder pressure measurements were collected over 300 consecutive cycles and an average of the 300 cycles is used in the analysis to help smooth out any variations. A standard calibration was performed to ensure accurate data acquisition [21]. Due to the

importance of the in-cylinder pressure data, care was taken to remove higher frequency noise. This was accomplished by applying a low pass filter to minimize false data within the data set. The low pass filter specifications were determined so that the pressure derivative maximum associated with the combustion events were minimally affected in both peak value and width.

Multiple sets of measurements were recorded at each operating condition for use in each data set. Statistical analysis is performed using standard techniques [22] when suitable. Additionally, the engine set points and corresponding emissions measurements are shown in Table 3. The emission data will be used in a later section when a qualitative analysis comparing the predicted trajectory and emissions data is performed.

Table 3 – Summary of experimental emissions for cases shown. First 8 cases at 1400 RPM with same fueling rate. Last 2 cases at higher speeds and higher horsepower values

Figure Reference	BMEP (bar)	Injection timing (°bTDC)	EGR Rate (%)	Injection Pressure (bar)	NO (ppm)	FSN	CO (ppm)	HC (ppm)
Figure 10	2.1	8	0	816	351	0.075	112	30
Figure 11	2.4	8	50	816	45	1.07	640	66
Figure 12	2.2	8	0	500	218	0.38	124	25
Figure 13	1.7	8	0	1500	568	0.022	101	18
Figure 14	1.8	0	0	816	220	0.014	825	164
Figure 15	1.2	0	50	816	3.8	0.04	4189	2019
Figure 16	1.1	0	50	500	2.2	0.5	3521	3141
Figure 17	1.4	0	50	1500	11.1	0.017	2670	746
Figure 18	5.6	9	0	1192	466	0.28	100	10.7
Figure 19	11.3	13	13	1254	350	1.22	140	6.8

The following summarizes the significance of each test case shown in Table 3 and later discussed in the main results section. The conditions in Figure 10 represent a conventionally timed injection with medium injection pressure and no EGR. This condition represents a baseline for comparison to other conditions in the paper. The operating conditions in Figure 11 are similar to Figure 10, other than the EGR rate which is now at 50%. The addition of EGR was the next

step in reducing harmful NOx emissions, this represents typical soot-NOx trade-off as evident by the experimental emissions results. The next step is represented in Figure 15 with retarded injection timing, the same 50% EGR rate, and the same medium injection pressure. In this case the NO is maintained low, while the soot is reduced significantly – this represents a low temperature combustion condition. Figure 12 and Figure 13 illustrate the effects of different injection pressure when compared to Figure 10, while Figure 16 and Figure 17 show the effects of different injection pressure on Figure 15. Figure 14 is presented for comparing the effects of retarding injection timing when compared to Figure 10. Figure 18 and Figure 19 represent higher speed and higher load cases and are presented to determine the usefulness of the predictive model at higher RPM ranges and horsepower ranges.

SPRAY CONTROL VOLUME EQUIVALENCE RATIO, TEMPERATURE, AND MASS OF FUEL BURNED TIME PROGRESSION DISCUSSION

The bulk of this section is presented as a means to understand the predictive model's spray variation in both axial and radial directions in terms of equivalence ratio, reaction temperature, and mass of fuel burned. The mapping of the burned fuel on the Φ-T plane will also be discussed. A time progression of the combustion process from the high speed, high load run is presented starting from 5% mass fraction burned, then 25%, 50%, 75%, 90% and ending at 97% mass fraction burned (which represents the end of combustion), This high speed, high load run has specific operating conditions of 2400 rev/min, 13% EGR rate, 1254 bar injection pressure and 11.3 BMEP.

The first figure shown, Figure 2, shows plots of the measured pressure, calculated bulk gas temperature, calculated heat release rate, and mass fraction burned. These plots are very useful were comparing the effects of different operating conditions with respect to combustion phasing, duration, intensity, and bulk gas temperature effects. The cylinder pressure plot (solid black line in Figure 2A) shows the data collected for experiments over the crank angles where combustion is occurring. The bulk gas temperature (red dashed line in Figure 2A) shows the calculated temperature inside the cylinder. In this particular case, the maximum gas temperature is about 1700K right after end of injection, indicating that the fuel will have a higher initial temperature when computing the reaction temperature. The MFB plot (solid black line in Figure 2B) represents the calculated mass fraction burned as mentioned in an early section. The heat release rate (HRR) plot (red dashed line in Figure 2B) in this case, shows a relatively small spike

early in combustion. This initial peak is usually characterized by premixed combustion leading up to the peak and then a more diffusion like flame until end of injection (EOI). In cases with lower loads, the initial premixed peak is often the most intense part of the combustion event. This is discussed more in the spray temperature discussion later in the section. These figures are presented here as an example of how the routine progresses and will be discussed in more detail when comparing the outcomes of multiple operating conditions.

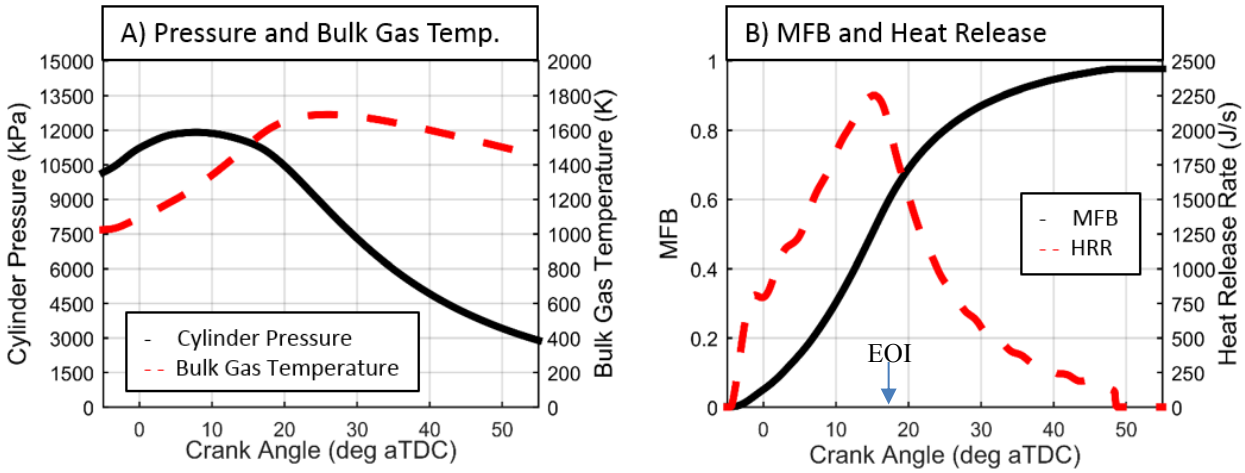

Figure 2 – A) Pressure and Bulk Gas Temperature and B) Mass Faction Burned and Heat Release Rate for operating conditions; injection timing at 13 deg. bTDC and 1254 bar injection pressure with 13% EGR rate

The next figure presented, Figure 3, represents the equivalence ratio within the fuel spray. The maximum value in the color bar was chosen to ensure the majority of the spray had distinct colors. This does not mean that the actual maximum equivalence ratio is six. Figure 3A occurs right after the start of combustion while fuel injection is still occurring. There are very high equivalence ratios in the center of the spray close to the injector tip while fuel is being injected. The equivalence ratio decreases as it moves further away from the injector tip and away from the centerline. As the model gets to the edges of the spray, there is a jagged edge due to fact that some of low equivalence ratio fuel is being burned off. In Figure 3B, fuel injection is still occurring and because of this, the equivalence ratio is still very high close to the injector tip. But

at this point in the time progression, the equivalence ratio at the edge of the spray has increased to around 1. This is due to the fuel below Φ equal to 1 burning up earlier in the combustion processes during the portion of the heat release that would typically be called the premixed combustion phase. By 25% MFB in Figure 3B, the flame has achieved a quasi-steady condition whereby the edge of the unburned portion of the spray is nearly a stoichiometric equivalence ratio that remains visible until peak heat release. By 50% MFB, show in Figure 3C, fuel injection has ended and the fuel next to the tip is becoming leaner as the fuel propagates into the cylinder. The effect of the air entrainment wave described by Musculus et al [14] can be seen in this figure where there is a slightly leaner mixture between the injection tip and the end of the spray (noted by red dashed line). The equivalence ratio time progression of the combustion process seen in Figure 3D, E, F represent ever decreasing values as more fuel is burned off until combustion is complete. At these points the combustion mode is transitioning from a standing diffusion flame in which the fuel moves toward the flame front to a condition where the reaction zone moves into the fuel rich regions.

The next step in the predictive model is to determine the mass of fuel burned in each control volume. These calculated values are represented in Figure 4. In Figure 4A, there is a relatively small amount of fuel being burned as evidenced by the color scale to the right of the plots. Most of the fuel in Figure 4 plots is fuel that farther away from the injector tip. This is a result of the spray model approach in which the spray is broken down into equal length sections in the axial direction and then gradually larger and larger widths in the radial direction as the spray expands. This means that the largest control volume is always at the tip of the spray. Combine this with the assumed Gaussian radial fuel distribution and the largest fuel mass is always in the center of the fuel spray. The diffusion flame front can be inferred in Figure 4A and

B where there is slightly more fuel burning towards the edges. There is also a relatively small amount of fuel being burned in the high equivalence ratio portions of the spray closer to the injector tip due to the percent heat release calculation discussed in the model summary section. That being said there are some parts of the spray centerline where more fuel is burning despite the richer mixture because there is simply more fuel in those cells than in the outer edges (smaller percent, based on kinetics results, of a larger number could end up being large). This holds true for the rest of the combustion process shown in Figure 4B, C, D, E, and F.

As stated earlier, the reaction temperature can be determined once the equivalence ratio is calculated. The reaction temperature associated with the spray are presented in Figure 5. By comparing the equivalence ratio and reaction temperature plots, it can be seen that, as expected, the hottest temperatures occur where the equivalence ratio is closest to stoichiometric. The initial premixed combustion mode is seen in Figure 5A where some of the fuel below the stoichiometric equivalence ratio is burning at a lower temperature near the edge of the spray. The diffusion flame mode is seen in Figure 5B where the outmost portion of the flame is burning at the hottest temperature. In Figure 5C, the flame is beginning to transition from the quasi-steady standing diffusion flame to the reaction front moving inwards, consuming the richer fuel towards the center of the spray. Figure 5D, E, F, the spray is continuing to burn inwards until the end of combustion.

Figure 6 is presented as example of a very different operation condition where injection timing is later at 8 deg. bTDC, injection pressure is lower at 816 bar, and EGR rate is much higher at 50% and BMEP is significantly lower at 2.4 bar. This constitutes a low speed, low power conventionally timed medium pressure injection. Figure 6 shows how much cooler the flame is overall when the EGR rate is considerably higher. This operating condition also

represents a condition where fuel injection is complete by the time combustion begins. In this case there is no clear standing diffusion flame front, except briefly in Figure 6C, and the primary combustion mode is the reaction front moving inward towards this center of the spray.

Now that the equivalence ratio, reaction temperature, and mass of fuel burned in each control volume has been determined, the ignition locations and combustion trajectories can be plotted on the Φ-T plane. By comparing these two plots, trends of the fuel moving across the Φ-T plane can be determined and observations of NOx and soot formation can be made. Figure 7 represents the conditions on Φ-T plane where fuel is first reacting in the combustion process. This is essentially a colored histogram of fuel amounts based on Figure 4, placed into bins based on Figure 3 and Figure 5. There is a limit to the burning temperature that is known based on the equivalence ratio of the burning fuel. This limit can be in seen in Figure 7A (offset dotted red line).This limit only moves as the pre-reaction temperature increases which is assumed to follow the bulk gas temperature determined as shown in Figure 2. This is why the plot values are moving toward hotter temperatures throughout Figure 7.

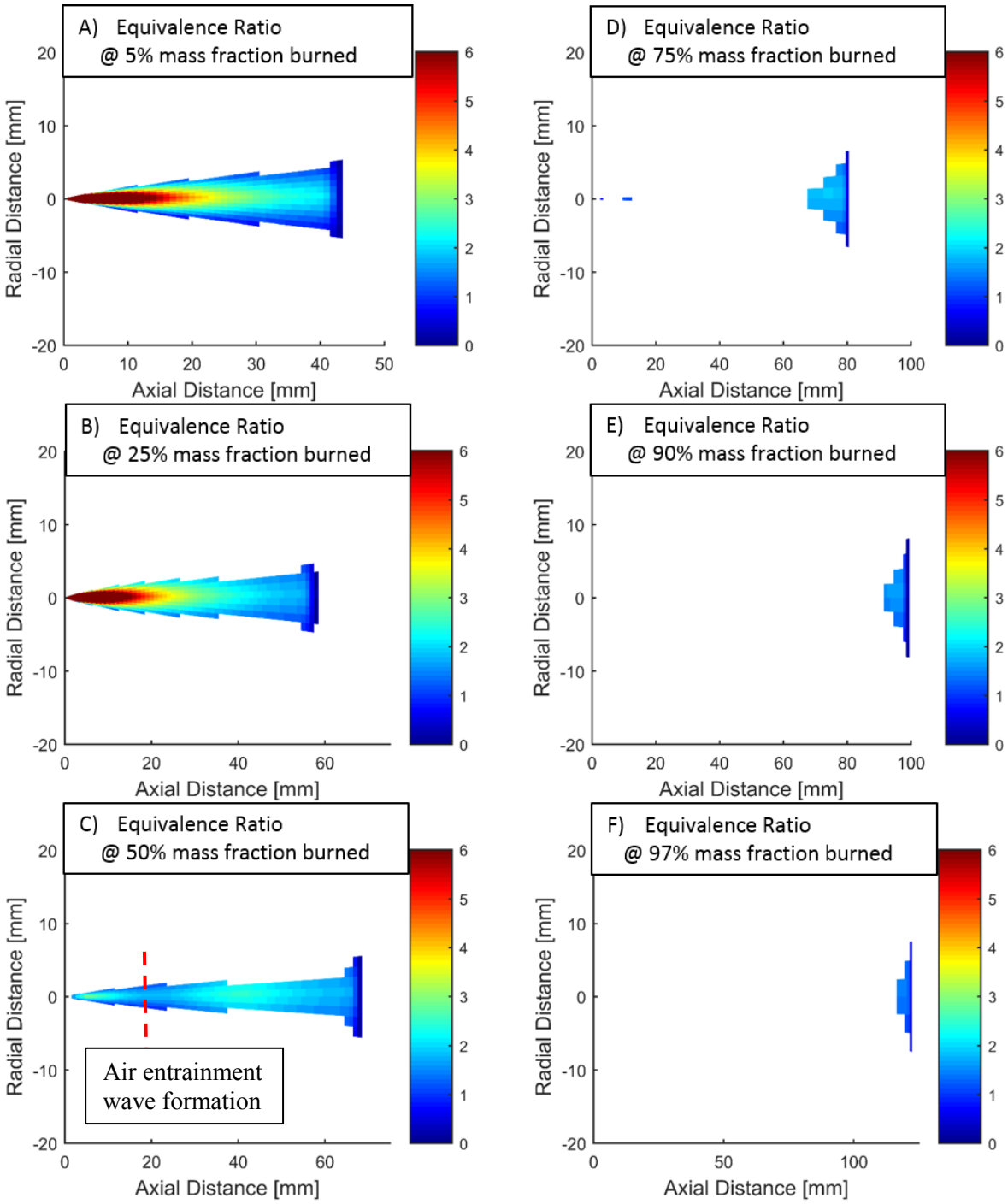

Figure 3 – Time Progression of Equivalence Ratio; injection timing at 13 deg. bTDC and 1254 bar injection pressure and 13% EGR rate

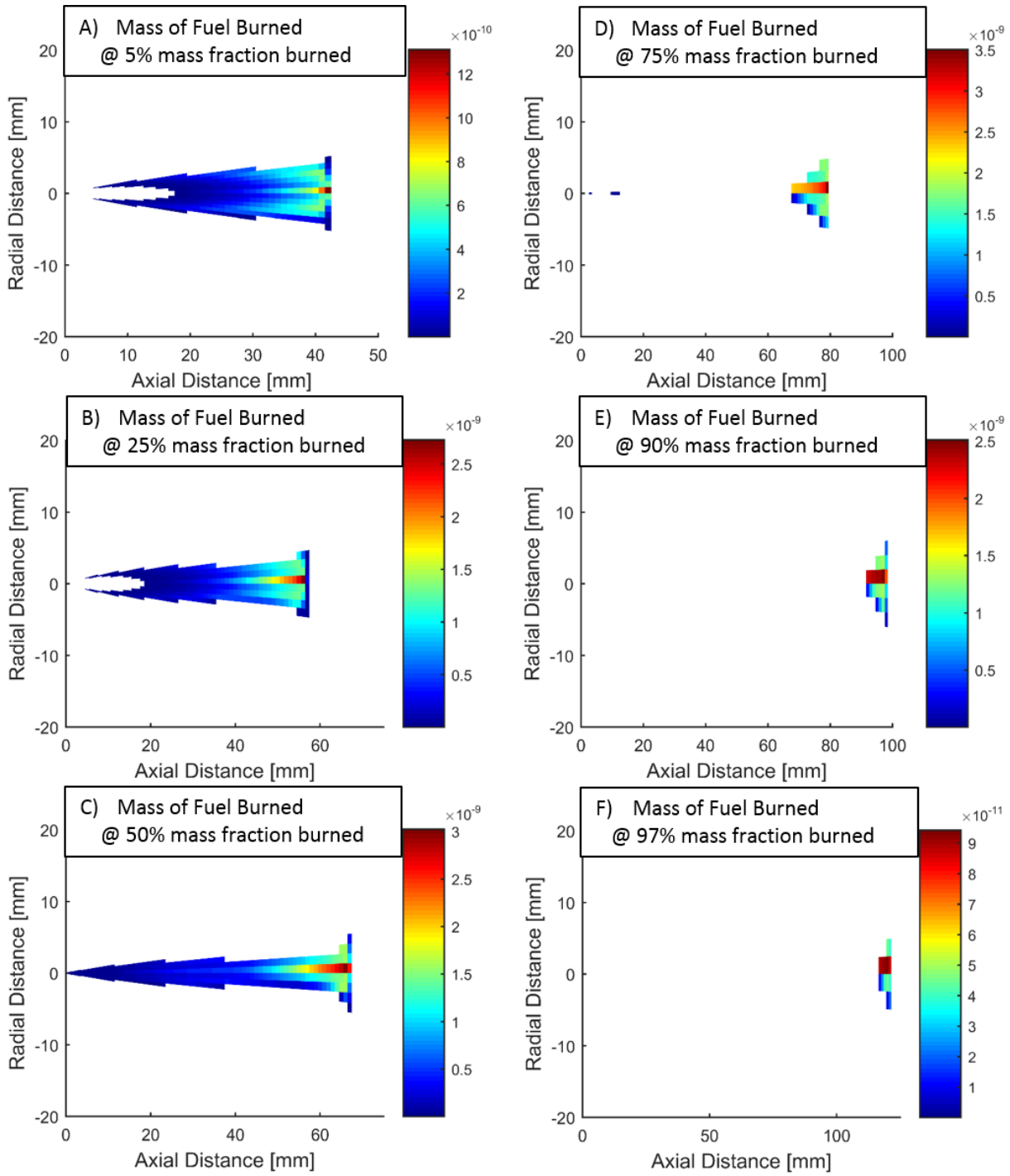

Figure 4 – Time Progression of mass of fuel burned; injection timing at 13 deg. bTDC and 1254 bar injection pressure and 13% EGR rate

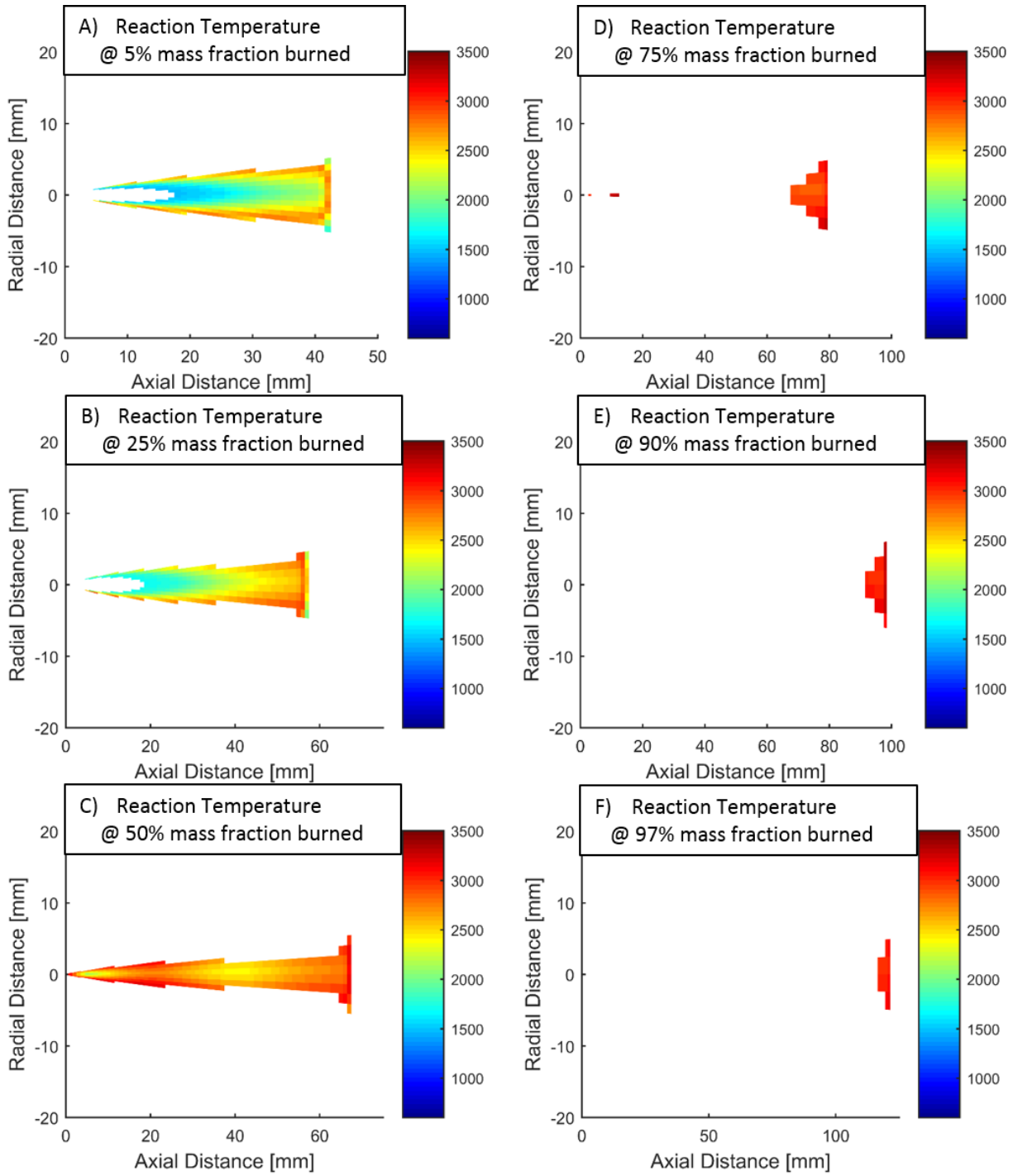

Figure 5 – Time Progression of Reaction Temperature; injection timing at 13 deg. bTDC and 1254 bar injection pressure and 13% EGR rate

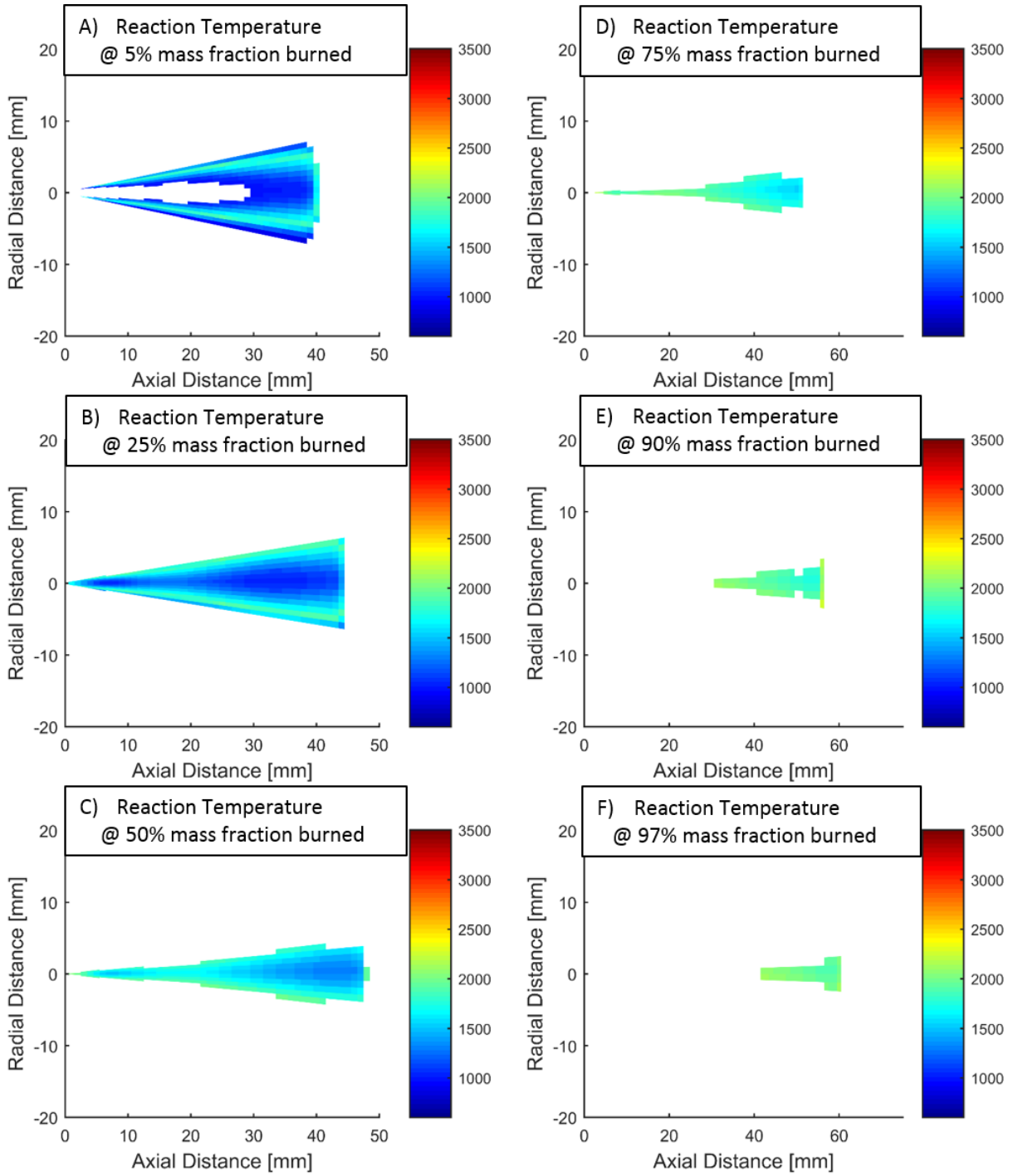

Figure 6 – Time Progression of Reaction Temperature; injection timing at 8 deg. bTDC and 816 bar injection pressure and 50% EGR rate

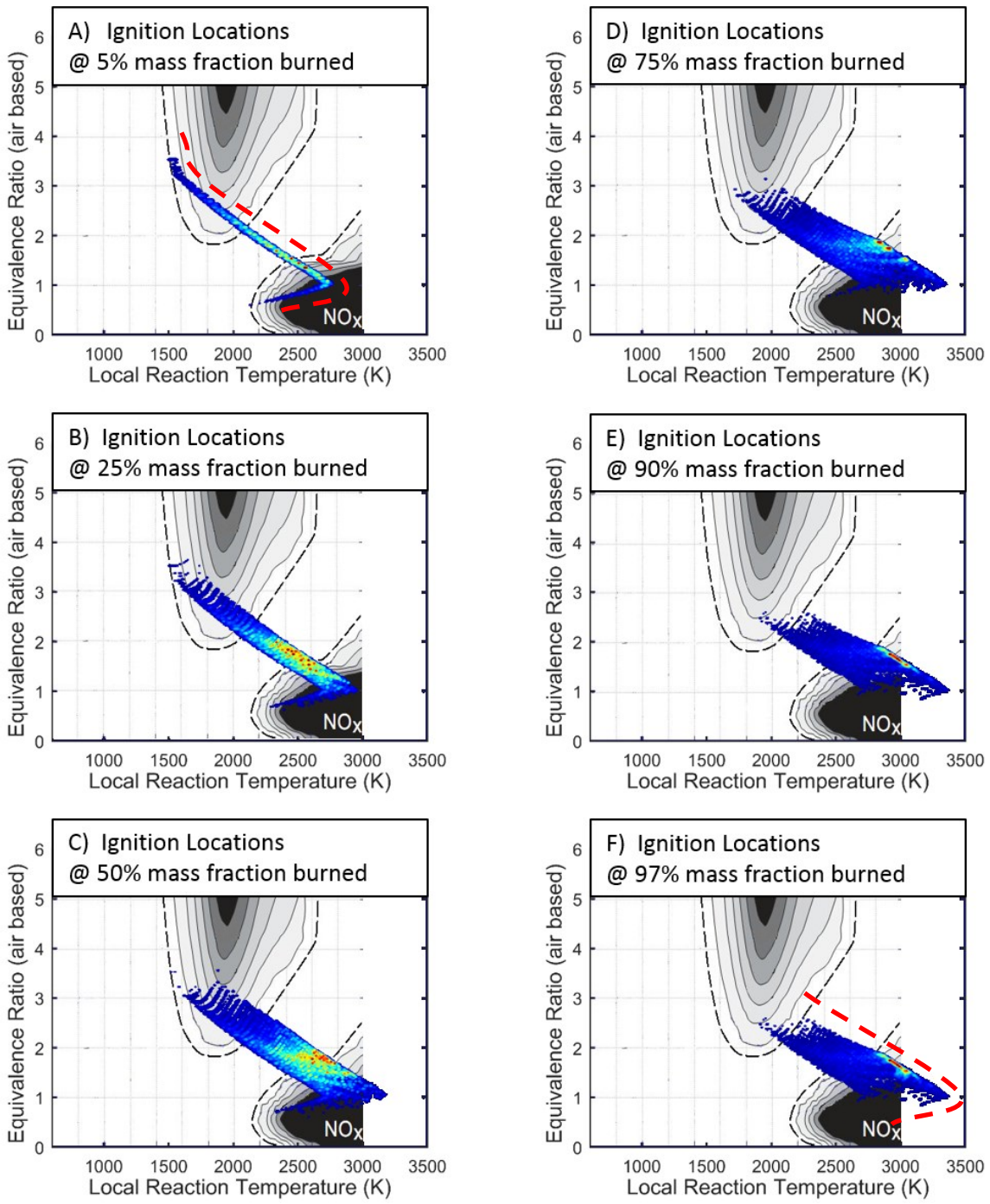

Figure 7 – Time Progression of Ignition Locations; injection timing at 13 deg. bTDC and 1254 bar injection pressure and 13% EGR rate

Figure 8 shows a history of the equivalence ratio and reaction temperature throughout the combustion process up to the point in time the plot was created. Early in the combustion process, the ignition locations plot and post ignition heating and cooling look very similar due to diffusion like flame structure where fuel is burning at a consistent equivalence ratio and hence a very similar temperature. After the standing diffusion flame stage ends and the reaction region starts to move inward towards the center of the spray and the reaction rate decreases, the previously burned fuel is able to mix and move down on the Φ-T plane (indicated by dotted red circle in Figure 8D). The reaction temperature is also observed to decrease due to the expansion cooling of the bulk gas (reference Figure 2A, bulk gas temperature begins to decrease around 25 deg. aTDC and 75% MFB.) which moves the fuel toward cooler temperatures on the Φ-T plane (indicated by dotted red arrow in Figure 8E). From these figures, it can be observed that much of the fuel is igniting at conditions within the NOx region and mixes and cools as combustion comes to and end but still remains in the NOx region. This observation coincides with the high NO measurements in the validation data.

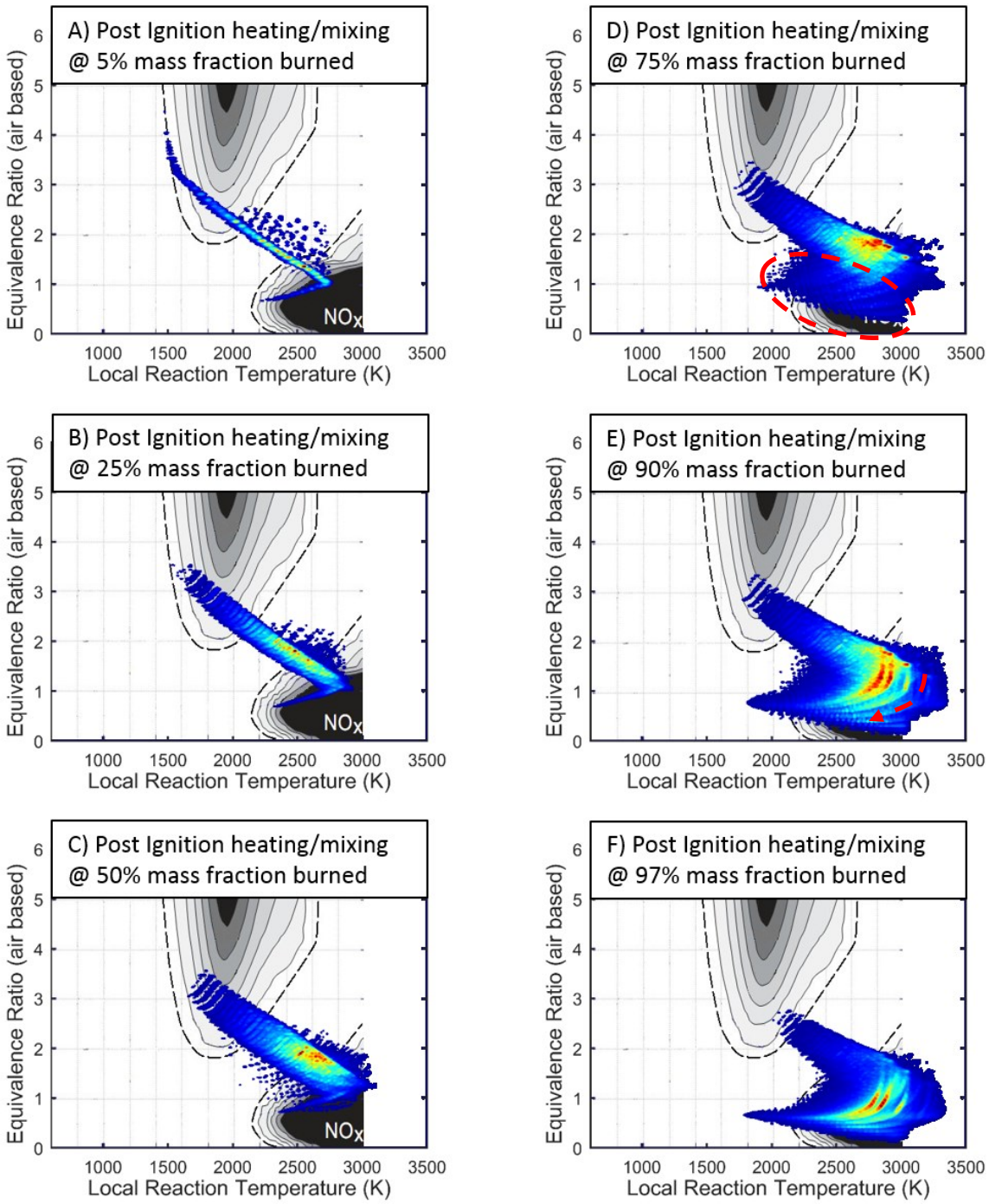

Figure 8 – Time Progression of Heating and Mixing; injection timing at 13 deg. bTDC and 1254 bar injection pressure and 13% EGR rate

Figure 9 references the example of a very different operation condition where injection timing is later at 8 deg. bTDC, injection pressure is lower at 816 bar, and EGR rate is much higher at 50% and BMEP is significantly lower at 2.4 bar. This constitutes a low speed, low

power conventionally timed medium pressure injection. It can be observed that the temperatures are much lower from combustion, hence the majority of the fuel is shifted to the left on the Φ-T plane. Much of the fuel is reacting in the soot formation region and then falling directly down as seen when comparing Figure 9C and Figure 9D (indicated by red arrow in Figure 9D. This indicates that it is not heating and possibly not oxidizing the soot being formed which can account for the very high filter smoke number. More observations and postulation regarding the emissions formation processes are made in a later section while this section is presented to explain the model outputs and what the information is available when discussing the observations. The trajectories in the remainder of the paper represent the state of the entire combustion event (i.e. at end of combustion or frame F in the figures above) at multiple different operation conditions showing the effect of injection timing, EGR, and fuel rail pressure in various combinations.

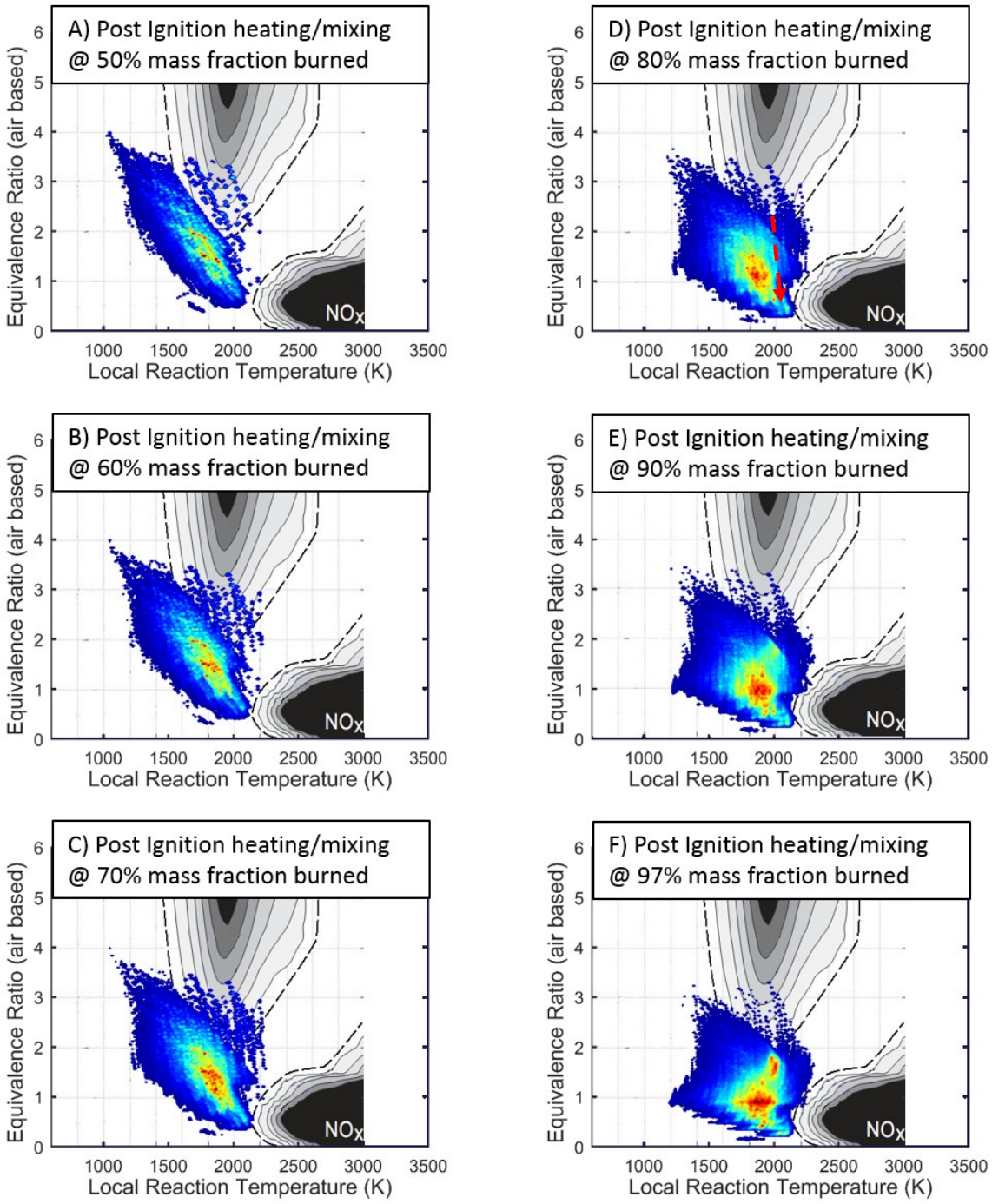

Figure 9 – Time Progression of Heating and Mixing; injection timing at 8 deg. bTDC and 816 bar injection pressure and 50% EGR rate

PREDICTED COMBUSTION TRAJECTORIES FOR VARIOUS OPERATING CONDITIONS

Conventional Combustion Mode

More description of the overall scheme of combustion trajectories is offered in evaluating the first operating condition, allowing the major differences to be highlighted for the remaining test conditions. The figure for each operating point consists of four plots. The top left plot (A) represents the measured cylinder pressure and inferred bulk gas temperature. The top right plot (B) represents the calculated heat release rate and mass fraction burned. The heat release plot is a common method for describing and comparing combustion events and will be used to interpret the proposed model. The bottom left plot (C) represents the fuel mass concentration at initial ignition conditions. The ignition locations illustrate how the fuel in the spray initially reacts throughout the combustion process. The high mass concentration areas indicate the conditions where the majority of the fuel starts reacting. The bottom right plot (D) represents the post ignition mixing and heating (or cooling) of fuel by the end of combustion.

By comparing the ignition points and overall mixing history, any heating (or cooling) behavior can be observed as the fuel continues to mix until the end of combustion. This trajectory can lead to insight about potential emissions formations (i.e. soot forming, but perhaps not oxidizing). Postulations such as that are purely speculative at this point, but enabling that discussion is part of the long term motivation for this modeling approach.

Figure 10 shows the results of the model for a conventional low load operating condition with a single injection at eight crank angle degrees before top dead center (8°bTDC) and no

EGR. The rail pressure is set at a mid-range value of 816 bar based on the stock ECU set point. This conventional low load condition is typically characterized by a well-mixed and therefore hot burning combustion event. This results in high NOx formation and low soot formation. The overall shape of the ignition location plot in Figure 10C correlates well to the expected results with most fuel being well mixed and reacting close to stoichiometric and burning hot in the NOx formation region. Due to the short combustion duration, the fuel does not experience much heating therefore the ignition locations are relatively static (points do not move very far to the right on the Φ-T plane)

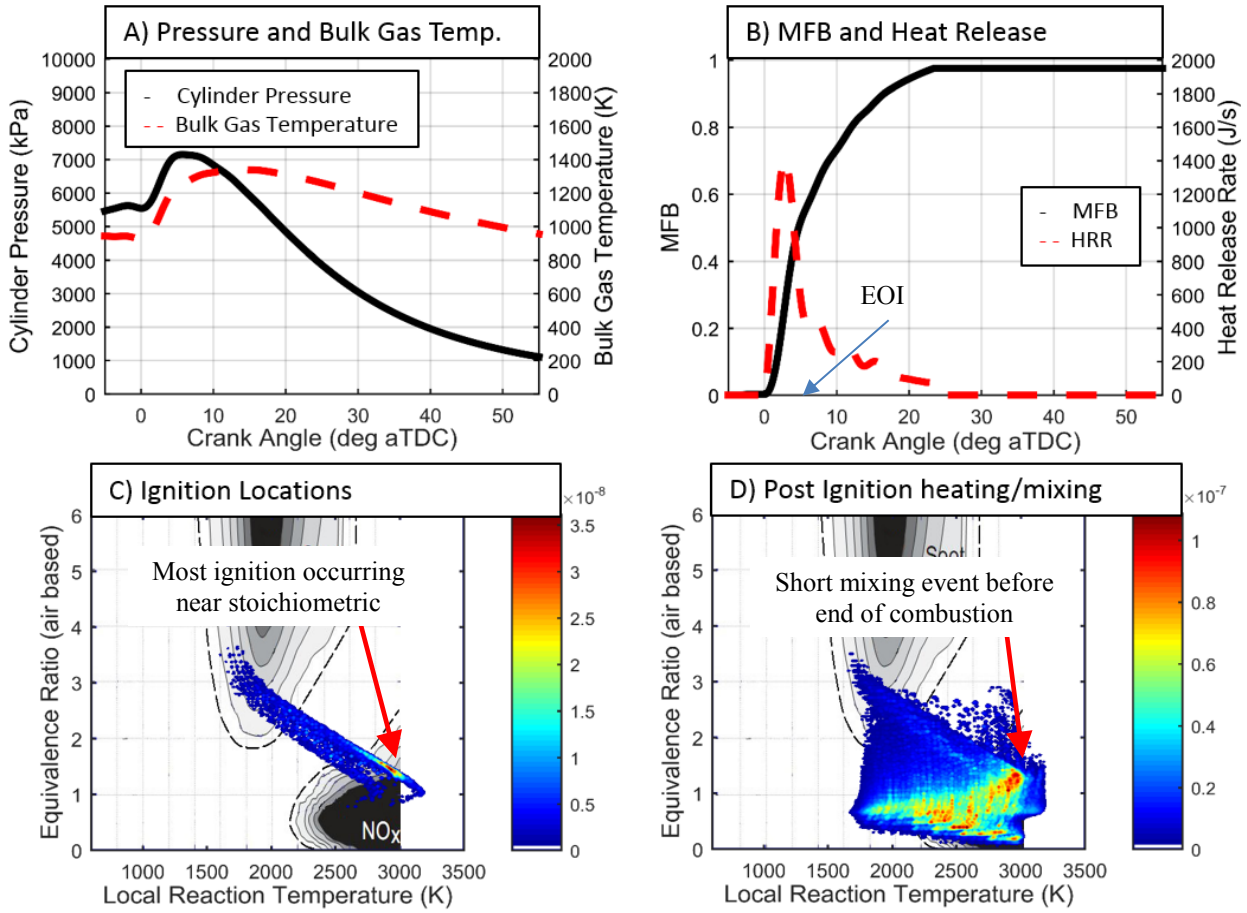

Figure 10 – Model results for conventional timing at 8 degrees bTDC 0% EGR, and 816 bar injection pressure

The overall results of the combustion process are represented in Figure 10D. There is a high mass concentration area close to 3000K and slightly above Φ = 1.0, or stoichiometric. This is due to the fuel that initially reacted around stoichiometric equivalence ratio mixing slightly, but not experiencing much bulk cooling (as seen near end of combustion in Figure 10A, but generally staying at very similar conditions near initial ignition locations. The other high mass concentration areas represent fuel that ignited early in the combustion process and mixed down on the Φ-T plane without heat substantially. The mixing to a lean condition of this fuel would likely allow time and temperature to oxidize any soot that is formed (notice combustion phasing in Figure 10A). There is some bulk cooling due to combustion phasing after top dead center

(expansion cooling), but the short duration keeps this to a minimum. The majority of the fuel at the end of combustion has been at a very high temperature (above 1800K) so NOx formation occurs very readily. This supports the expected, and observed high NO emission measurement.

Care is taken to avoid too much speculation at this point about any direct emissions predictions. However, it is the intention of the author at this stage to demonstrate the potential application of this type of model to provide insight into the combustion and emissions formations at least qualitatively. The experimental emissions results for this and remaining test conditions are provided in an earlier section and discussed briefly in the next section.

Figure 11 shows the results for the high EGR case (50%) with other parameters (i.e., injection timing and rail pressure) remaining unchanged. EGR levels this high represent those commonly seen in low temperature combustion modes (but perhaps with different injection timings) and will be used in comparison to such cases. When introducing EGR, the NOx formation is expected to decrease while soot production would increase. The heat release curves of Figure 10 and Figure 11 show small differences in intensity and phasing, but the reaction temperatures are lower due to a large EGR rate. This is due to the overall equivalence ratio throughout the spray being higher due to less air in the mixture. The lower reaction temperature also keeps the bulk gas temperature slightly lower, lowering the reaction rate in future time step calculations. In Figure 11C, the initial ignition high mass concentration area is at a much higher equivalence ratio, Φ=2, and a much lower temperature, 2000K. Notice that this high mass concentration area is just inside the soot formation region. Based on the global equivalence ratio, there is approximately 40-50% less oxygen in the cylinder when high EGR rates are applied at a consistent fueling rate (this is true for all low load EGR cases presented in this paper). This fact and the mixing and cooling indicates that the soot that was initially formed will not be able to

oxidize due to the lower temperature and lack of oxygen. The fuel that was burned close to the start of injection was initially well mixed and continued to mix and heat as the bulk gas temperature increased. This caused a slight push to the NOx formation zone in Figure 11D. This could be a contributing factor to why conventional timing produces more NOx than late timing low temperature combustion as the retarded injection timing further suppresses NOx formation.

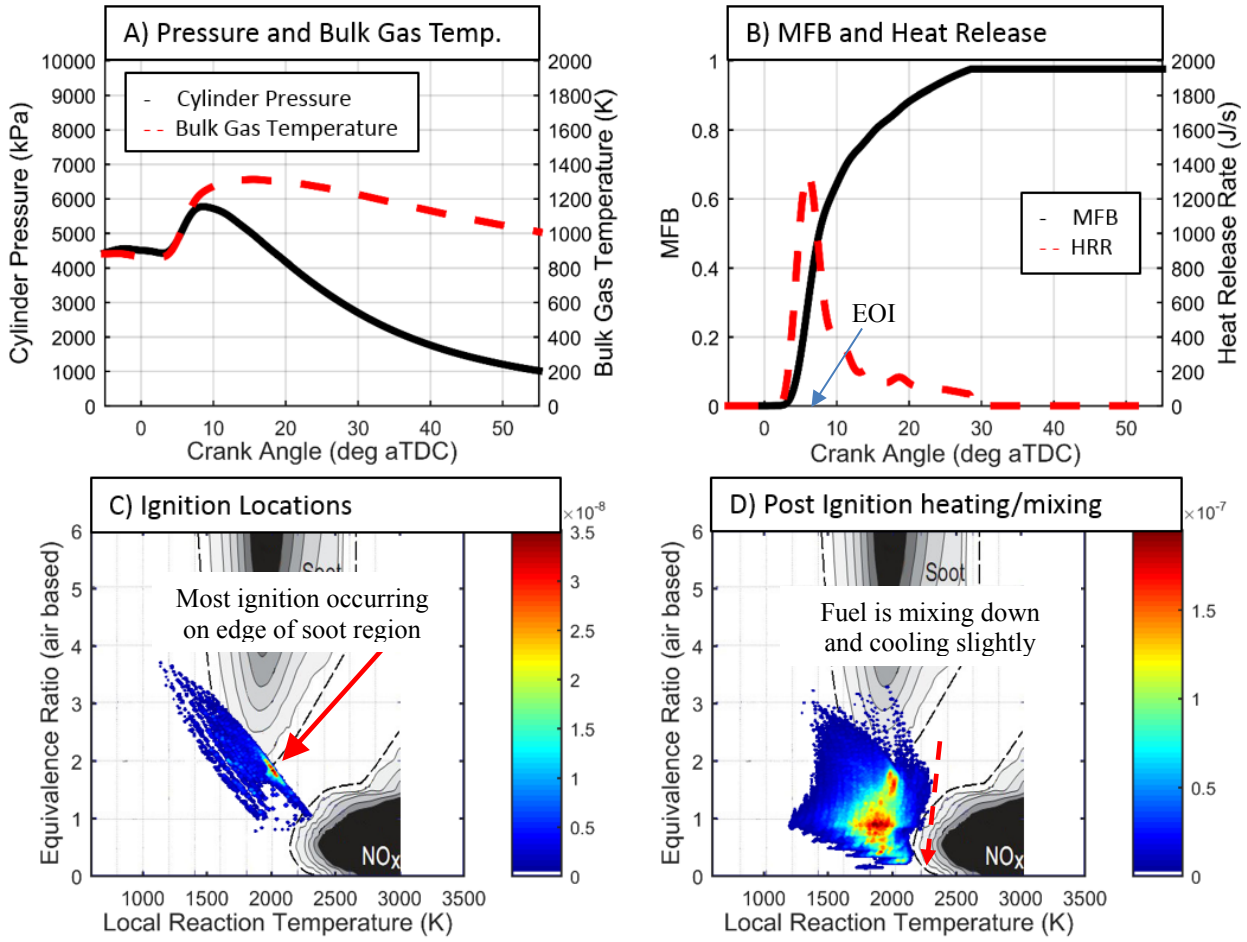

Figure 11 – Model results for conventional timing at 8 degrees bTDC 50% EGR, and 816 bar injection pressure

Figure 12 and Figure 13 show the effects that rail pressure has on the predicted trajectory for conventional injection timing and no EGR. Recall that that previous iterations of this model were not able to adequately capture rail pressure influences on the trajectory [13].

The plots in Figure 12 represent a conventional combustion event at 500 bar rail pressure. The combustion duration is observed to be slightly longer while the phasing is similar to the first case (Figure 10). There is a slight difference with a lower intensity reaction close to the beginning of the heat release curve seen in Figure 12B. The high mass concentration areas at initial ignition in Figure 12C occur at slightly richer conditions due to the increased injection duration resulting from the lower pressure. The post mixing plot shows a general trend towards mixing without much temperature change. The fuel is still at a very high temperature similar to the first case and this may explain why most of the soot that formed when some fuel ignited within the soot formation region is oxidized (note that there is not a well-defined soot formation cutoff as indicated by the dashed line around the soot region).

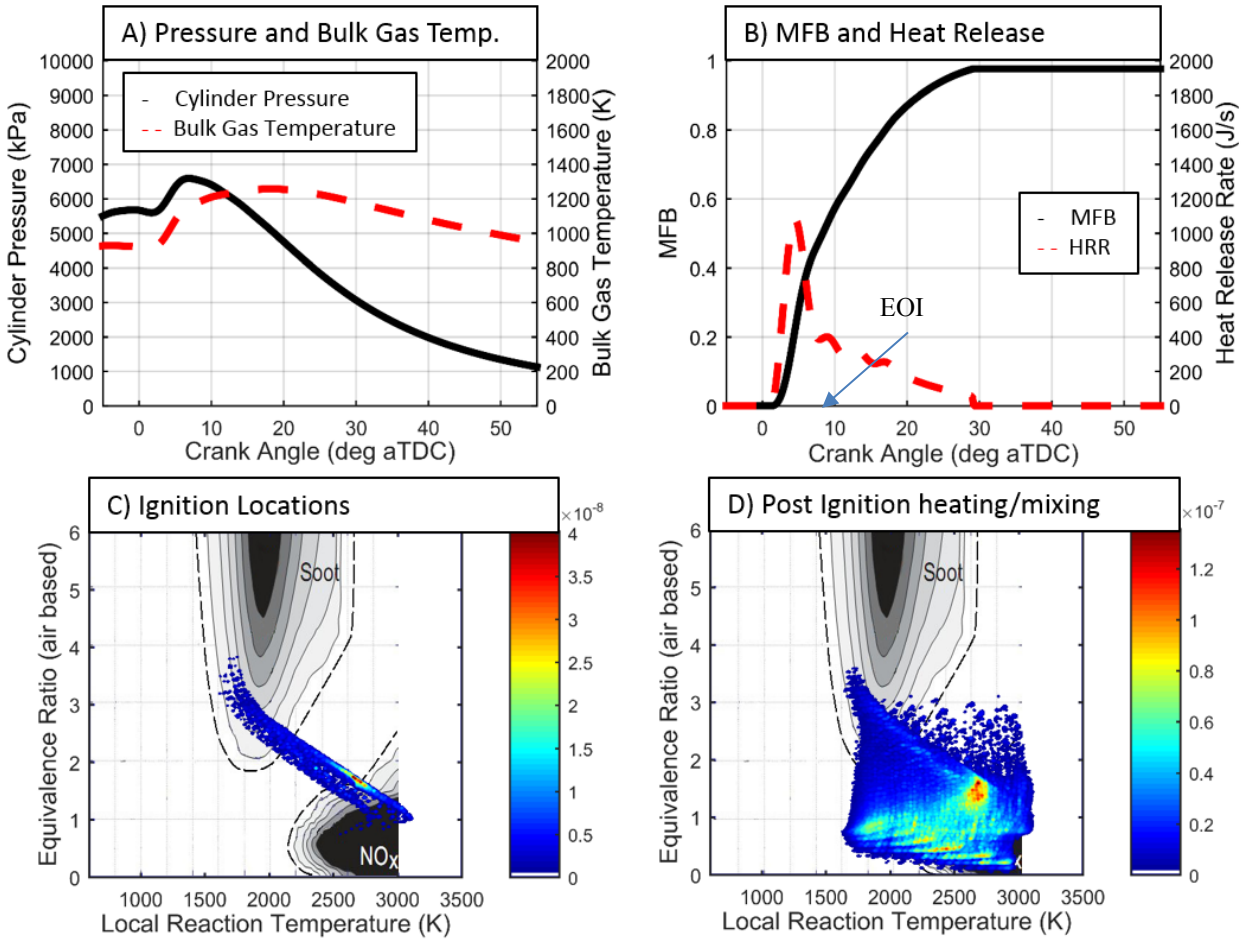

Figure 12 – Model results for conventional timing at 8 degrees bTDC 0% EGR, and 500 bar injection pressure

The plots in Figure 13 represent a conventional combustion event at 1500 bar rail pressure. The combustion duration at this higher injection pressure is much shorter with higher intensity, likely due to accelerated mixing resulting from faster injection velocities and subsequent increased air entrainment. The enhanced mixing leans out the mixture slightly and moves the high concentration area down on the Φ-T plot compared to the low injection pressure combustion trajectory. This conventional combustion operating condition also shows a slight continued heating during post mixing in Figure 13D which matches from the bulk gas temperature increase during combustion seen in Figure 13A. This trend in concert with the higher reaction temperatures, due to the lower equivalence ratio and high bulk gas temperature,

likely leads to more complete soot oxidation and higher NOx concentration (notice trajectory in Figure 13D has moved even further into NOx region compared to Figure 12D).

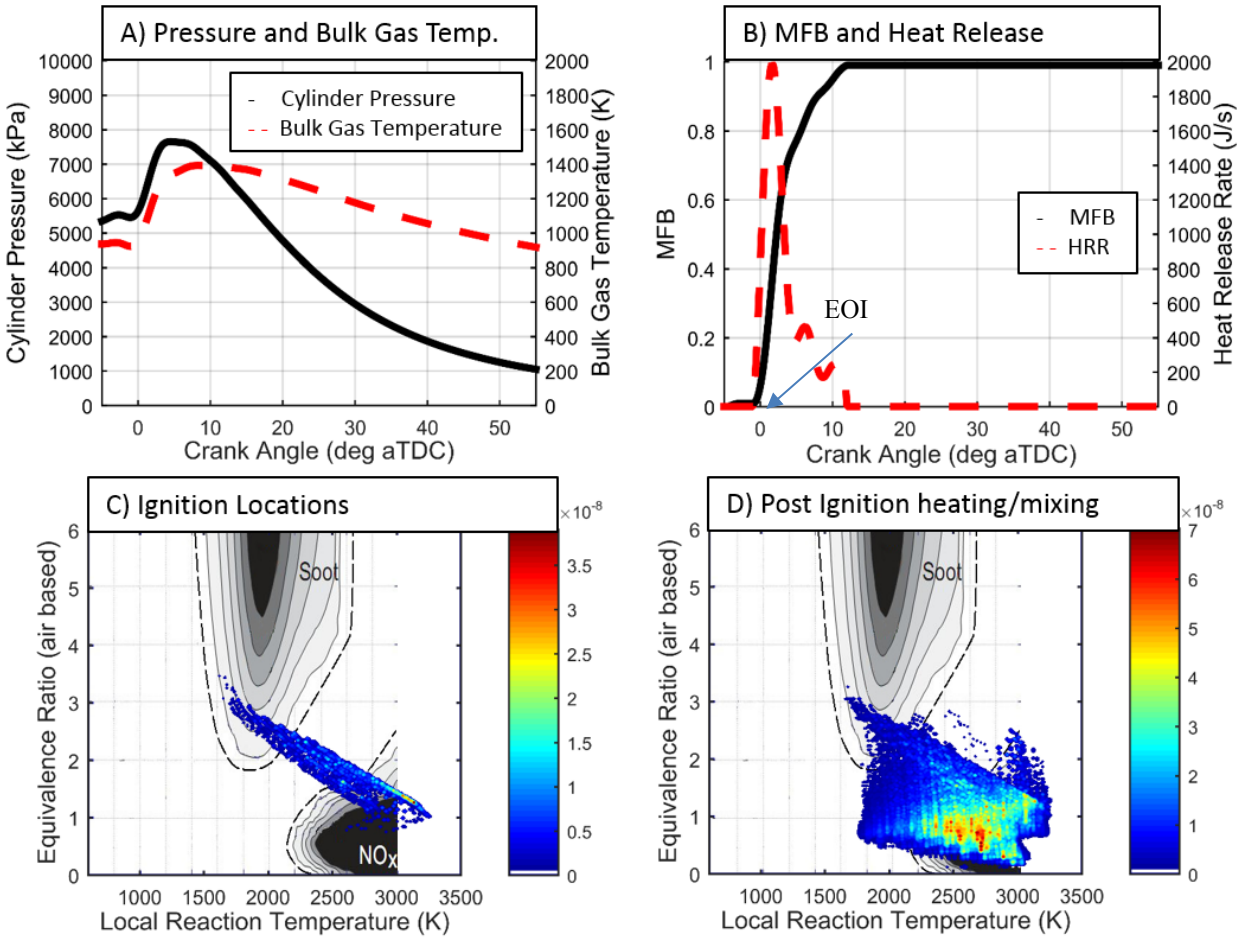

Figure 13 – Model results for conventional timing at 8 degrees bTDC 0% EGR, and 1500 bar injection pressure

Low Temperature Combustion Mode

Figure 14 shows the results for a low temperature combustion operating condition with a single injection at TDC and a rail pressure of 816 bar. There is no EGR in this operating condition. Low temperature combustion (LTC) is an operating condition were fuel is injected, in this case, at a later crank angle in order to change the shape of the heat release rate enough to allow for increased mixing for fuel before combustion. This can lower the equivalence ratio, and thereby move the combustion trajectory away from the soot formation region. LTC is most effective when used in conjunction with high EGR rates at low load to lower NOx emissions and soot emissions. The operating condition in Figure 14 is not a very common combination but is presented for comparison between other conditions. The bulk gas temperature and heat release rate are very similar to the conventional mode in Figure 10, except that they are moved about 10 crank angle degrees later due to the later injection timing. The ignition locations are very similar when compared to the conventional plot. The post mixing plot shows a slight trend towards heating by the end of combustion, allowing for more complete soot oxidation but the high mass concentration area is still well within the NOx zone.

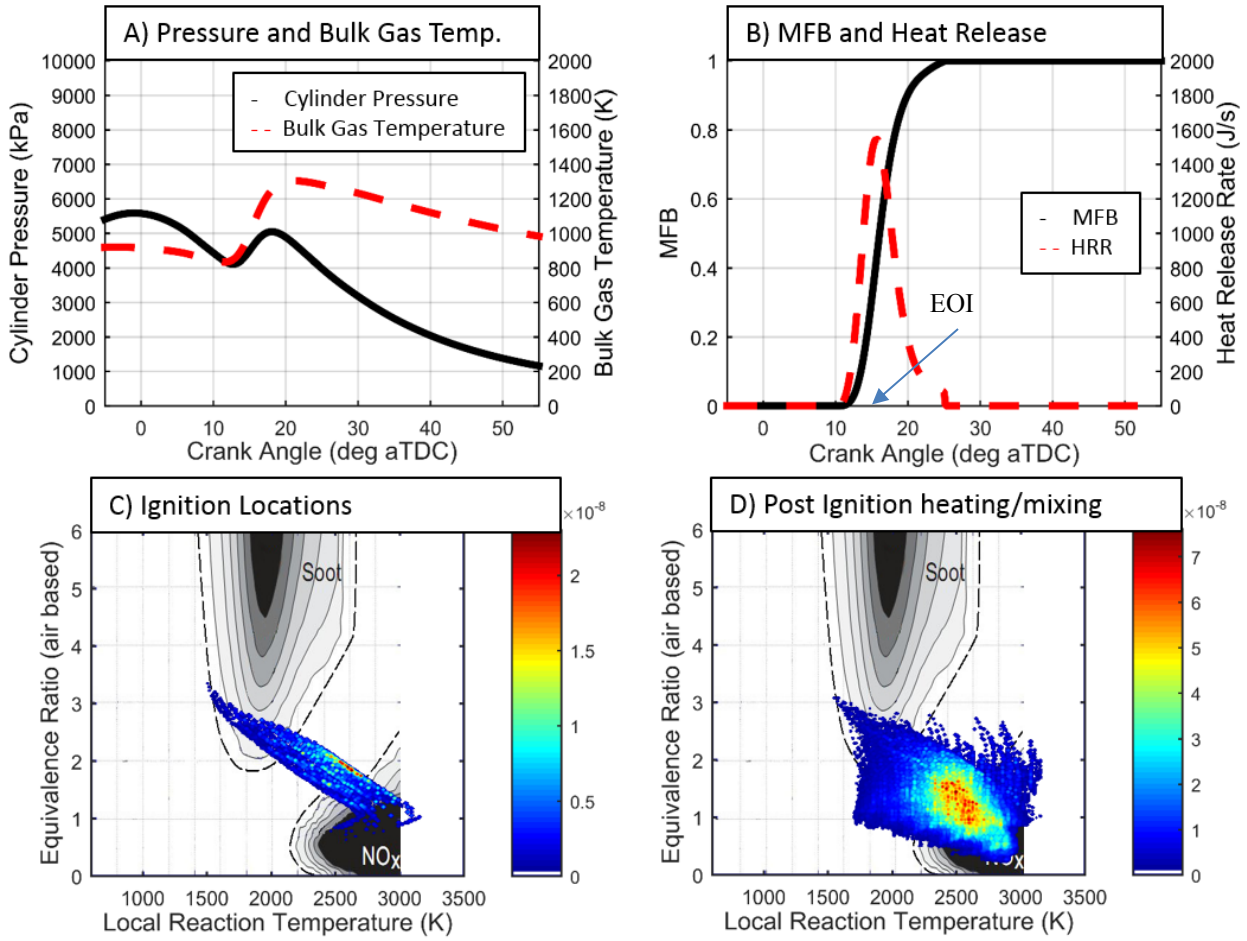

Figure 14 – Model results for LTC, timing at 0 degrees bTDC 0% EGR, and 816 bar injection pressure

The plots in Figure 15 represent a low temperature combustion operating condition with a single injection at TDC. The rail pressure remains the same and the EGR rate is 50%, meaning that injection timing is changed compared to the condition shown in Figure 11 and the EGR rate has changed when compared to Figure 14. The late injection and high EGR rate is used to delay ignition and combustion phasing to create the LTC operating condition. With LTC conditions, the bulk gas temperature stays lower than in conventional timing, which limits reaction temperature as evidenced by the mass concentration area at lower ignition temperatures, around 1700K (see Figure 15C). This could be an indicator of low temperature heat release, shown in Figure 15B, which can be seen to have two ignition stages. The lessened increase in bulk gas

temperature due to expansion keeps the high mass concentration during ignition away from the soot formation zone as compared to the conventional condition. Soot and NOx formation are controlled with low temperature combustion. The primary ignition equivalence ratio is approximately 1.75 (seen in Figure 15C) which is nearly identical to the conventional combustion with high EGR case shown in Figure 11C. The ignition delay before second stage heat release may account for some movement down away from the soot formation region. It appears that in this case, the primary mechanism for reducing soot in the LTC case is the reduced chamber temperature at ignition and subsequent cooling that occurs due to long combustion duration at later crank angles.

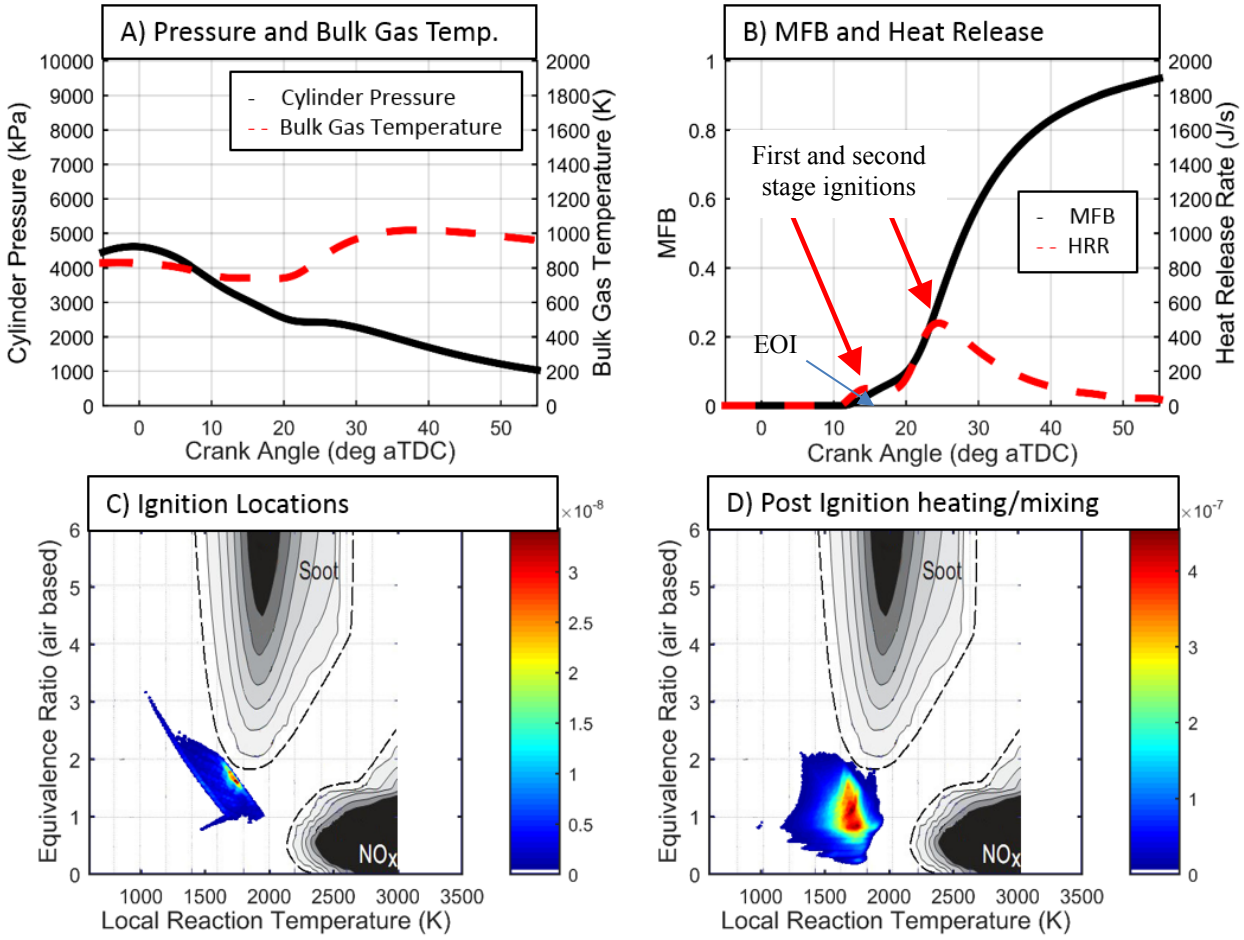

Figure 15 – Model results for LTC, timing at 0 degrees bTDC 50% EGR, and 816 bar injection pressure

Figure 16 and Figure 17 show the effects that rail pressure on the predicted trajectory in LTC operating conditions with 50% EGR rate. The plots in Figure 16 represent a low temperature combustion event at 500 bar rail pressure. The combustion duration is observed to be slightly shorter while only having similar peak intensity compared to Figure 15. There is a noticeable difference with a lower intensity first stage reaction close to the beginning of the heat release curve seen in Figure 16B. The high mass concentration areas at initial ignition in Figure 16C occur at much richer conditions due to the increased injection duration resulting from the lower pressure. The post mixing plot shows a general trend towards cooling with some possible soot formation occurring (note that there is not a well-defined soot formation cutoff as indicated by the dashed line around the soot region) and a reduced possibility of oxidation due to lower temperatures from late phasing and low reaction intensity. The soot formation would occur more readily in this operating condition due to the increased equivalence ratio caused by the change in the injection pressure when compared to higher rail pressure of Figure 16.

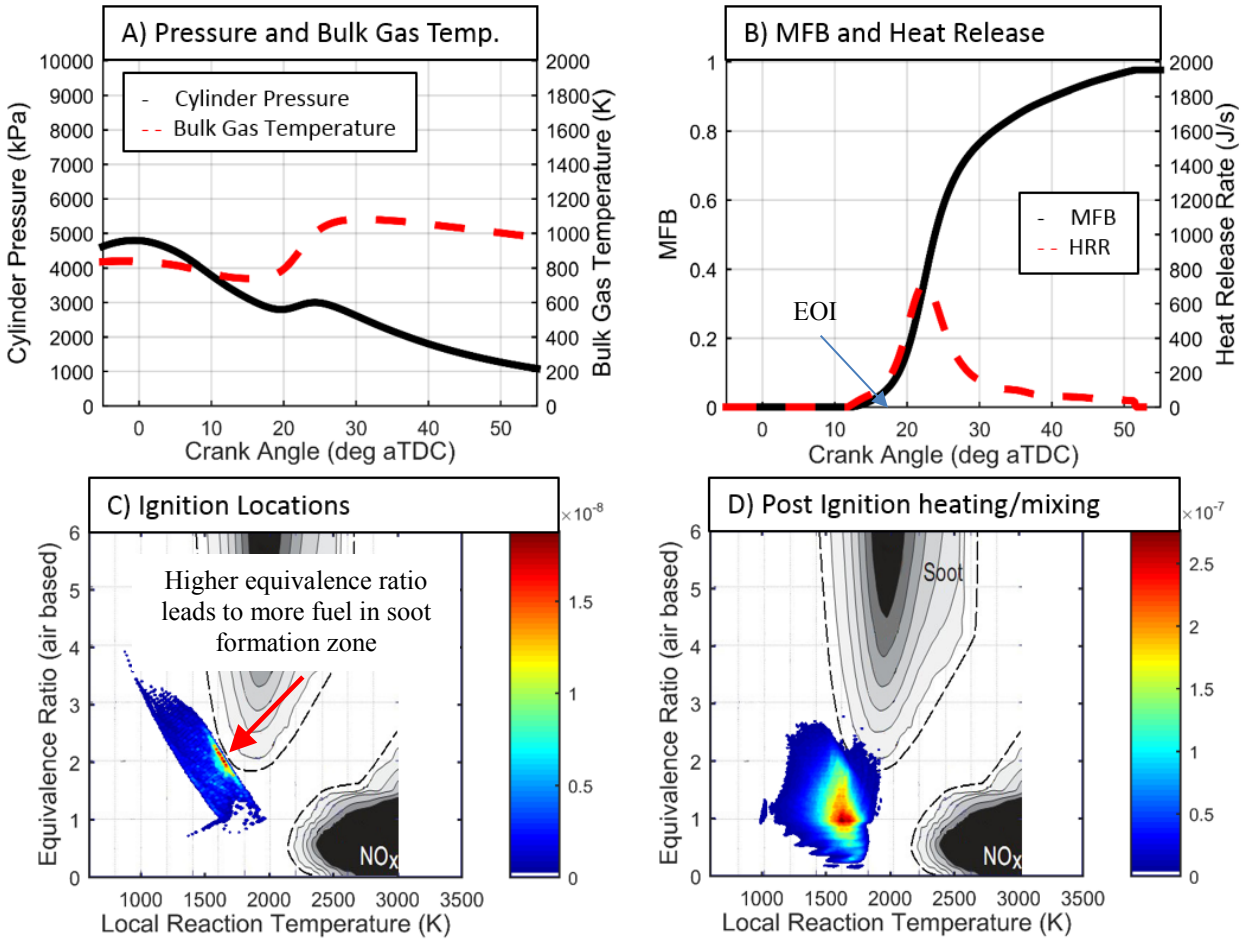

Figure 16 – Model results for LTC, timing at 0 degrees bTDC 50% EGR, and 500 bar injection pressure

The plots in Figure 17 represent a low temperature combustion event at 1500 bar rail pressure. The combustion duration at this higher injection pressure is decreased, likely due to accelerated mixing resulting from faster injection velocities and subsequent increased air entrainment. The enhanced mixing helps lean out the mixture and moves the high concentration area down on the Φ-T plot compared to the low pressure combustion trajectory. Due to the reduced equivalence ratio, the ignition temperature also increases significantly, moving the high mass concentration below and to the right of the tip of the soot formation zone with only a small amount of fuel within the soot formation zone. The higher heat release rate increases the bulk gas temperature, raising the reaction temperature as well. This low temperature combustion

operating condition shows a slight heating during post mixing. This can promote soot oxidation without heating enough to produce significant NOx. There is still some fuel concentration moving slightly into the NOx zone with the hotter temperatures.

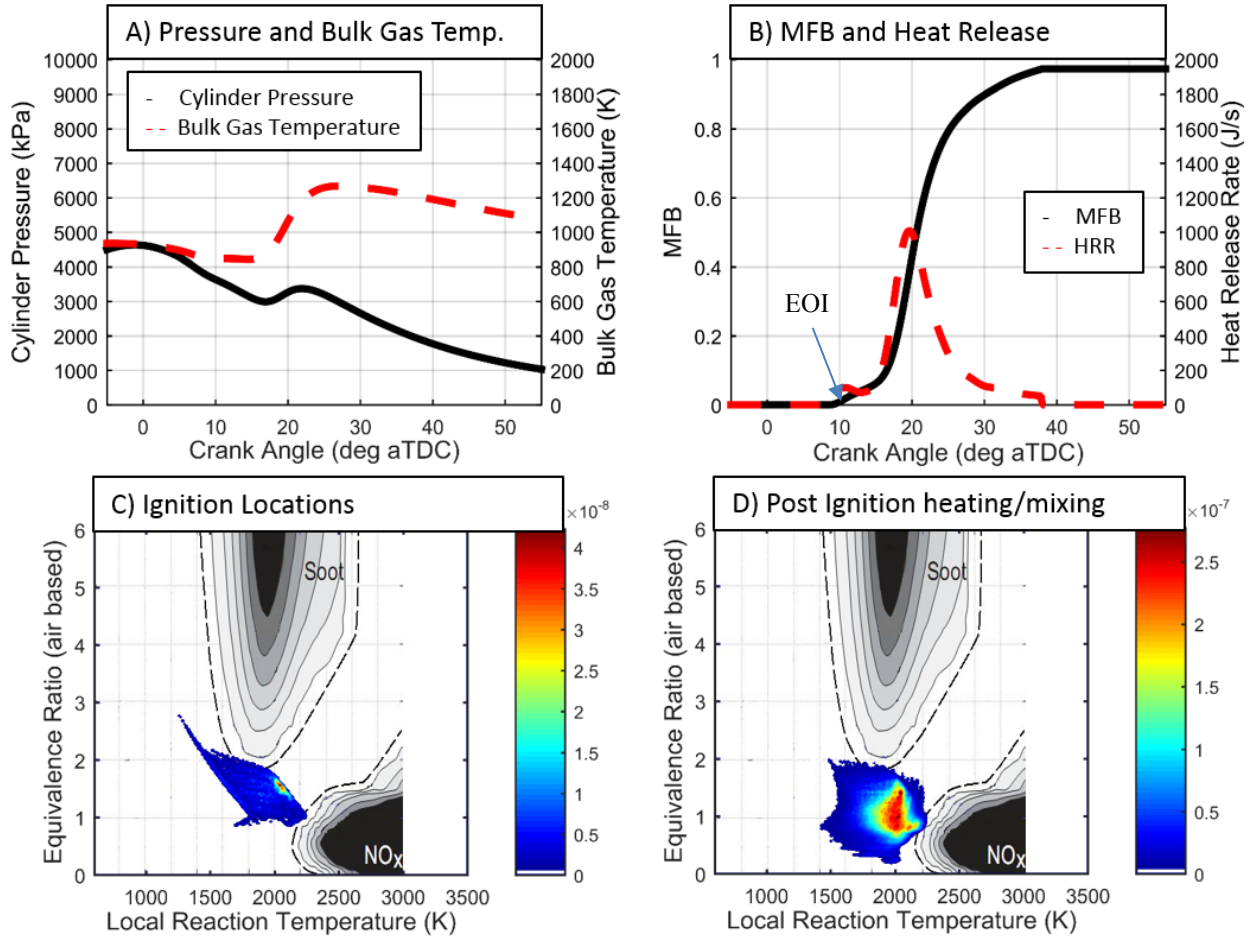

Figure 17 – Model results for LTC, timing at 0 degrees bTDC 50% EGR, and 1500 bar injection pressure

High Speed and High Torque Conventional Combustion Mode

Figure 18 and Figure 19 represent operating conditions that are radically different from the above conditions. These conditions constitute higher horsepower and higher engine speeds with parameters controlled by the stock engine controller parameters.

The plots in Figure 18 represent an operating condition at 1900 rpm and 5.6 bar BMEP (150 hp.) with injection timing at 9 degrees before TDC and 1192 bar injection pressure. There is no EGR associated with this operating condition. There is a first stage ignition that is very similar in intensity and phasing to the first conventional test condition (Figure 10). The bulk gas temperature, seen in Figure 18A is noticeably hotter than the other operation condition discussed so far, likely due to the increased fueling required to reach the higher load. The ignition equivalence ratio in Figure 18C is very similar to the first conventional condition (Figure 10) at Φ=1.5, but due to the hotter bulk gas temperature, the fuel concentration is shifted to the right on the Φ-T plane. In Figure 18D, the majority of the fuel has settled in the NOx zone. There is also a trend towards cooling as mixing occurs, suggesting that some soot formed in combustion process may not be oxidized. It is important to note that there is approximately 60% less oxygen in the combustion chamber when compared to Figure 10 which could impact the amount of soot that is oxidized.

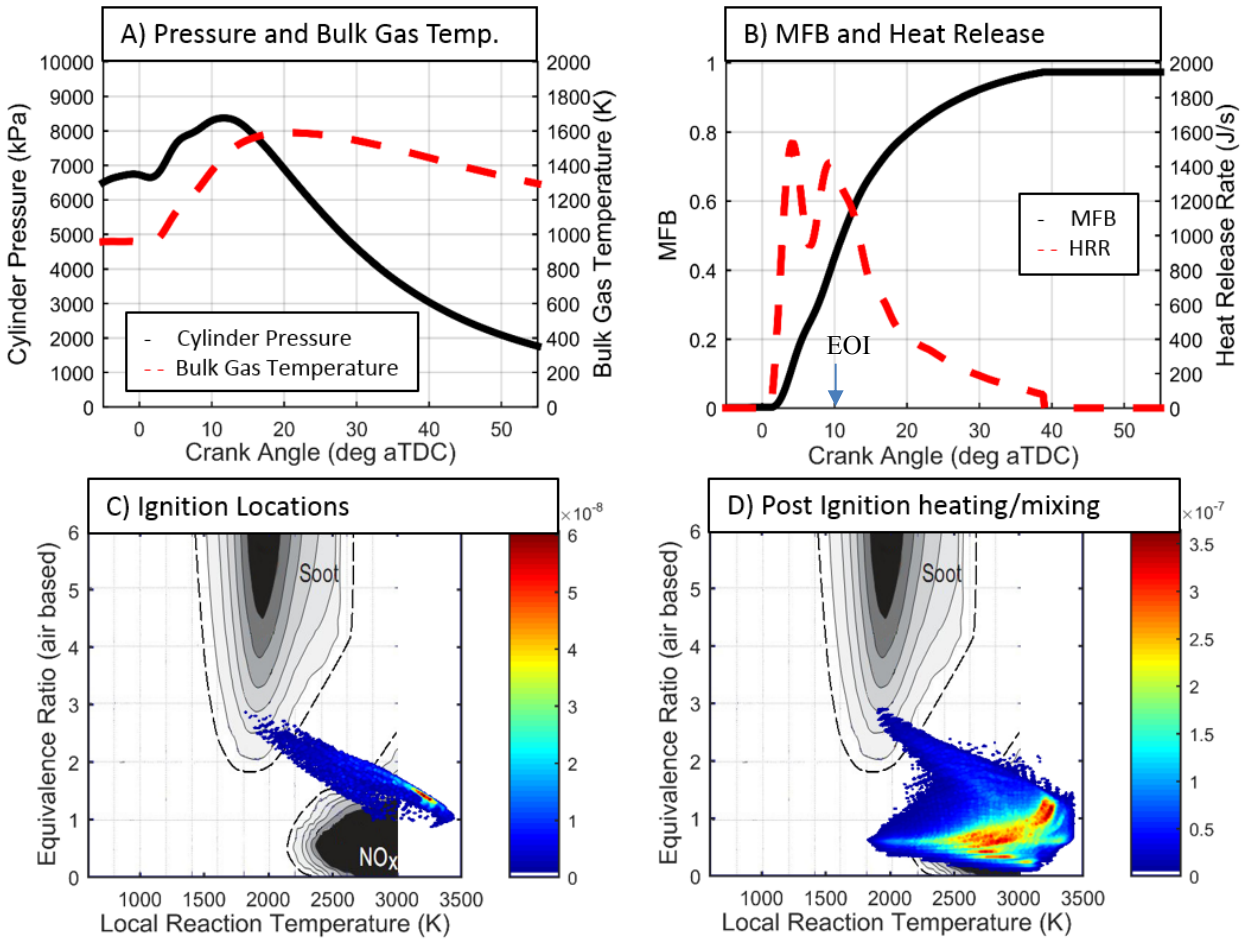

Figure 18 – Model results for conventional timing at 9 degrees bTDC 0% EGR, and 1192 bar injection pressure at 1900 rpm and 150 HP

Figure 19 represents an operating condition at 2400 RPM and 11.3 BMEP (300 hp.) The injection timing is set at 13 degrees before TDC and injection pressure is set to 1254 bar. The bulk gas temperature is slightly hotter than the operating condition in Figure 18. The heat release rate for this operating condition has a very long duration with a low intensity first stage and a very energetic second stage heat release (please note that the scale in Figure 19B is different from the other heat release rate plots in this thesis). The shape of the plot in Figure 19C is very similar to the ignition plots of the mediums speed operating condition with an exception to the high mass concentration area. The high mass concentration area occurs at slightly richer conditions and thus slightly lower temperatures in an area to the outskirts of the NOx zone

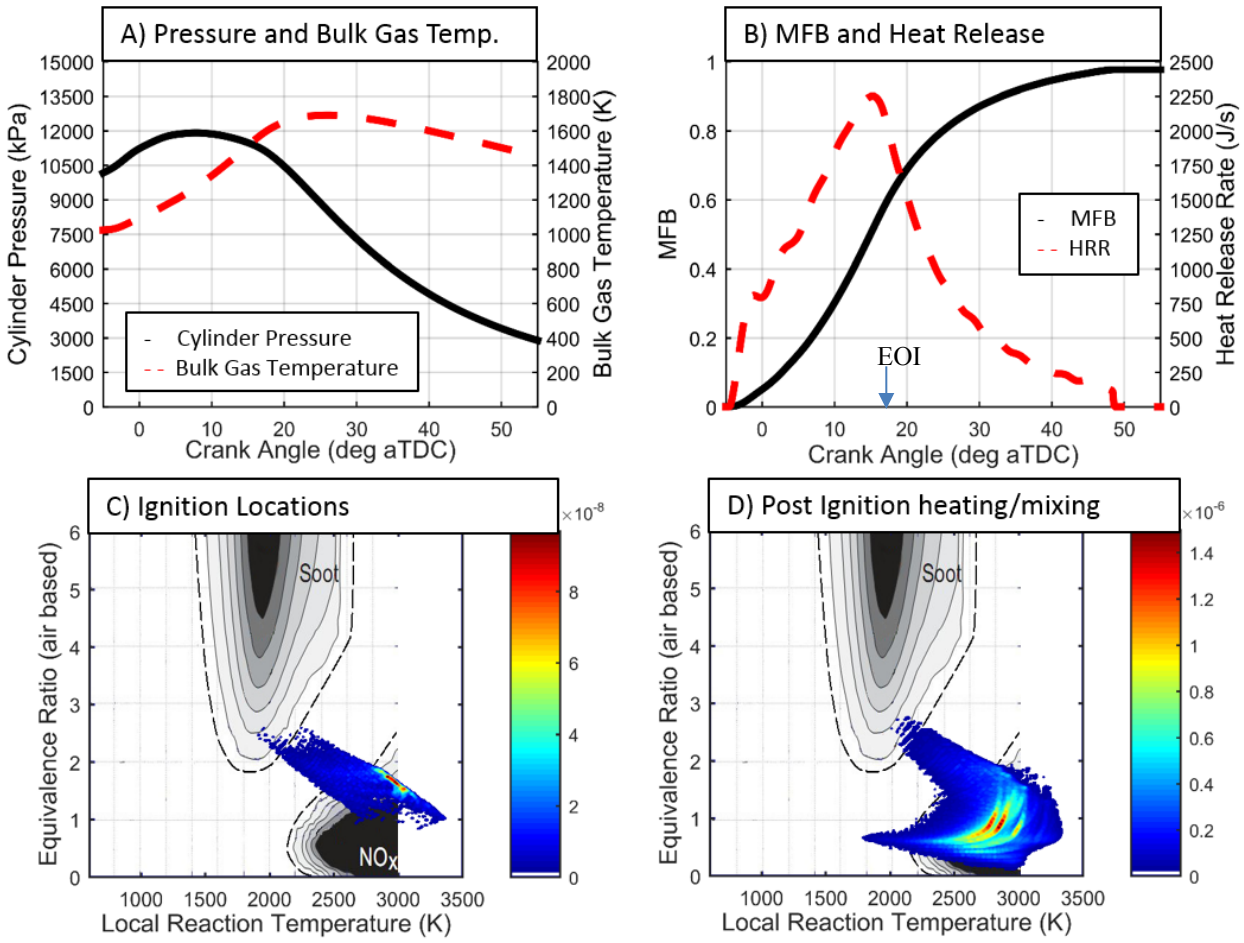

Figure 19 – Model results for conventional timing at 13 degrees bTDC 13% EGR, and 1254 bar injection pressure at 2400 rpm and 300 HP (note that the scale in B is different from other HHR plots)

instead of being directed in the middle of the zone like the medium speed condition. A large portion of the fuel in the post mixing plot is seen to mix down and cool as combustion comes to an end. This mass concentration area has some extremities which are close to the edge of the NOx zone while the majority fuel is directly in the NOx zone. There is a considerable amount of fuel that ignited early in the combustion process within the soot formation area. It is important to note that there is approximately 115% less oxygen in the combustion chamber when compared to Figure 10 due to the larger amount of fuel that must be injected to support the higher power operating conditions. This implies that there may be enough heat to oxidize some of the soot but

there may not be enough oxygen left within the cylinder. This could lead to higher FSN numbers in the higher horsepower cases where considerably more fuel is burned.

QUALITIATIVE COMPARISON BETWEEN COMBUSITON TRAJECTORIES AND EXPERIMENTAL RESULTS

Table 3 (shown below as well as in an earlier section) presents some key emissions measurements that were obtained during testing. These include NO concentration, filtered smoke number (FSN), CO concentration, and hydrocarbon (HC) concentration. This information is presented to facilitate a qualitative comparison between different testing conditions by comparing the values presented in Table 3 and the combustion trajectories.

Table 3 – Summary of experimental emissions for cases shown. First 8 cases at 1400 RPM with same fueling rate. Last 2 cases at higher speeds and higher horsepower values

Figure Reference	BMEP (bar)	Injection timing (°bTDC)	EGR Rate (%)	Injection Pressure (bar)	NO (ppm)	FSN	CO (ppm)	HC (ppm)
Figure 10	2.1	8	0	816	351	0.075	112	30
Figure 11	2.4	8	50	816	45	1.07	640	66
Figure 12	2.2	8	0	500	218	0.38	124	25
Figure 13	1.7	8	0	1500	568	0.022	101	18
Figure 14	1.8	0	0	816	220	0.014	825	164
Figure 15	1.2	0	50	816	3.8	0.04	4189	2019
Figure 16	1.1	0	50	500	2.2	0.5	3521	3141
Figure 17	1.4	0	50	1500	11.1	0.017	2670	746
Figure 18	5.6	9	0	1192	466	0.28	100	10.7
Figure 19	11.3	13	13	1254	350	1.22	140	6.8

Of particular interest is the rail pressure effect under low temperature combustion conditions. When comparing the emission values in Table 3, it is observed that the smoke number and NOx concentration for both the 816 bar and 1500 bar low temperature operating conditions are almost identical. However, the CO and HC concentration values are very different. The high pressure combustion trajectory indicates the possibility for more heating

during post mixing and significant high mass concentration area that propose better fuel oxidation efficiency. The increase in oxidation efficiency would lead to lower carbon monoxide and unburned hydrocarbon emissions. This effect cannot be directly observed on the soot-NOx formation plot, but can be inferred by the higher temperatures which more efficiently oxidizes the fuel. The CO and HC results may be discussed but are not used as validation from the combustion trajectory model.

In general, the overall expected trends in emissions based on above discussion are indeed observed. The conventional timing without EGR exhibits high NOx and low smoke. This corresponds to plots in Figure 10D where the mass concentration is far to the right (hot).The expected tradeoff between NOx and soot occurs with the addition of high EGR corresponding to Figure 11D where the mass concentration has moved to a more central location on the plot, outside the NOx zone. This move can be seen in Figure 20A and B. The fuel is not hot enough to oxidize as much of the soot that is formed. It would be expected that the soot (FSN) would be lower and the NO concentration to be higher in the no EGR case due the high temperatures as evidenced by the mass concentration areas in Figure 20. This is confirmed by the validations results which indicate that the no EGR operating conditions has a FSN of 0.075 and NO concentration of 351 parts per million (ppm) while the 50% EGR rate operating conditions has a FSN of 1.07 and NO concentration of 45 ppm.

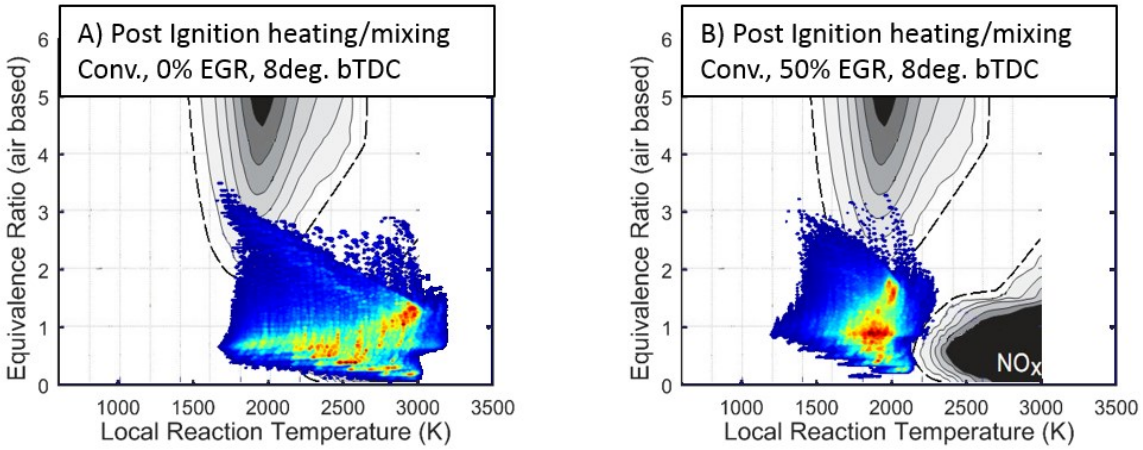

Figure 20 – Comparison of post ignition heating and mixing plots for conventional timing, 816 bar injection pressure at 0% and 50% EGR rates

When timing is moved later in the cycle without any EGR, the NOx concentration and FSN are similar to the conventional operating conditions and the post mixing plots look similar. When high EGR rate is added to a late injection timing condition, an LTC operating mode occurs which further reduces NOx and also lowers smoke below conventional combustion levels. This can be seen in Figure 15D with the mass concentration area being both outside the NOx region and soot formation region. The cooler temperatures can be seen when comparing the two plots in Figure 21. The fuel is not hot enough to oxidize as much of the soot that is formed. It would be expected that the soot (FSN) would be higher in the conventional case due larger amount of fuel in the soot formation area in Figure 21A when compared to Figure 21B. The NO concentration is expected to be lower in the LTC case where the high mass concentration area is further from the NOx formation area. This is confirmed by the validations results which indicate that the conventional operating conditions has a FSN of 1.07 and NO concentration of 45 parts per million (ppm) while the 50% EGR rate operating conditions has a FSN of 0.04 and NO concentration of 3.8 ppm.

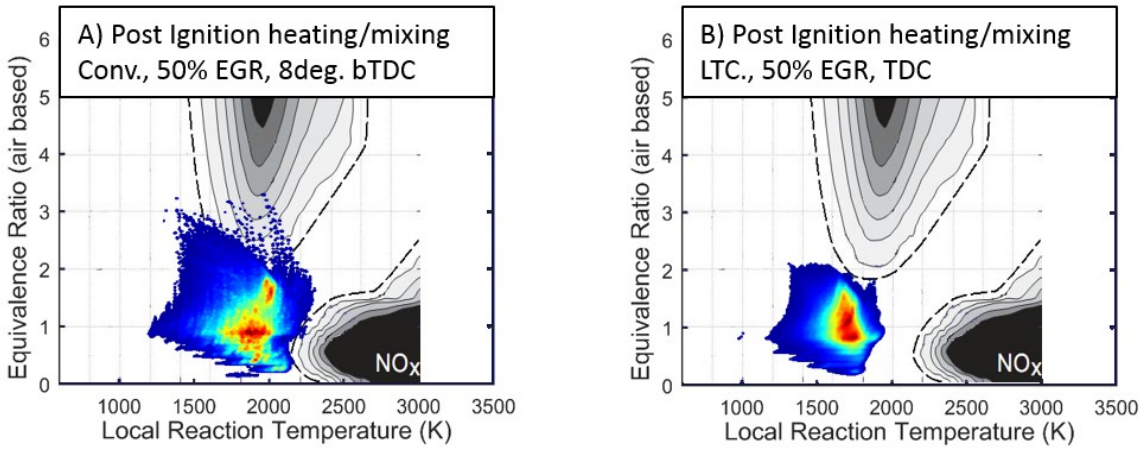

Figure 21 – Comparison of post ignition heating and mixing plots for 50% EGR rate, 816 bar injection pressure for both Conventional and LTC modes

For both conventional and LTC operating conditions, when the injection pressure is reduced, the FSN increases likely due to the richer mixtures that resulted from increased injection duration required to keep fueling rate the same. This also keeps the temperatures slightly lower, reducing the NOx concentration when compared to the corresponding medium injection pressure condition. The post mixing plots change to reflect these conditions by moving up and to the left slightly.

Conversely, as the injection pressure is increased, the FSN values decrease while the NOx concentration increases. This is likely due to the increased mixing and air entrainment that occurs as fuel is injected at higher pressures. With the lower equivalence ratios, the reaction temperature increases. This can be seen in the combustion trajectory plots as the mass concentration moves down and to the right slightly. As seen in the post mixing plots in Figure 22, the lower pressure conditions has a wider range of equivalence ratios while the higher pressure conditions exhibit a narrow equivalence ratio range with hotter temperatures. It would be expected that the soot (FSN) would be lower in the higher pressure case due to the smaller amount of fuel in the soot formation area and the NO concentration would be higher in the

higher pressure case due to the movement of the high concentration area closer to the NOx formation region. This is confirmed by the validations results which indicate that the low pressure operating conditions has a FSN of 0.5 and NO concentration of 2.2 ppm while the high pressure operating conditions has a FSN of 0.017 and NO concentration of 11.1 ppm.

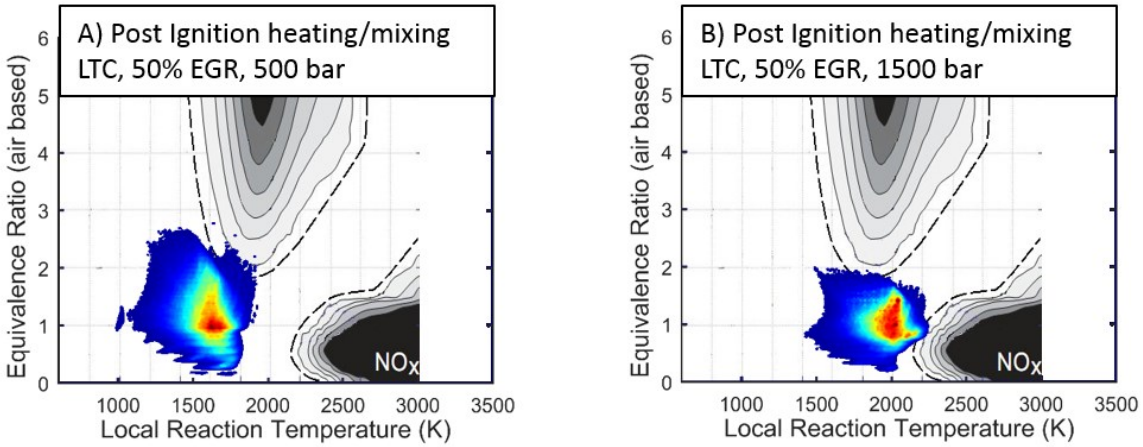

Figure 22 – Comparison of post ignition heating and mixing plots for 50% EGR rate, 816 bar injection pressure for both Conventional and LTC modes

At the higher power and speed conditions, the NOx concentrations are very high due to the high temperatures and lack of high EGR rate. The mass concentrations are well within the NOx zone. However, the FSN numbers are more difficult to correlate to a trend in the combustion trajectories. Early in the combustion event, there is a significant amount of fuel that is burning within the soot formation zone as seen in Figure 23. Due to the large amount of fuel that is injected during this operating condition, this fuel seems to "disappear" by the end of combustion plot. The lower relative oxygen concentrations to fuel in the combustion chamber means that there is less oxygen during combustion to oxidize soot that is formed early in the combustion event. It is also possible to see the cooling that occurs as the mass concentration starts in the red circle and moves down and to the right in Figure 23B.

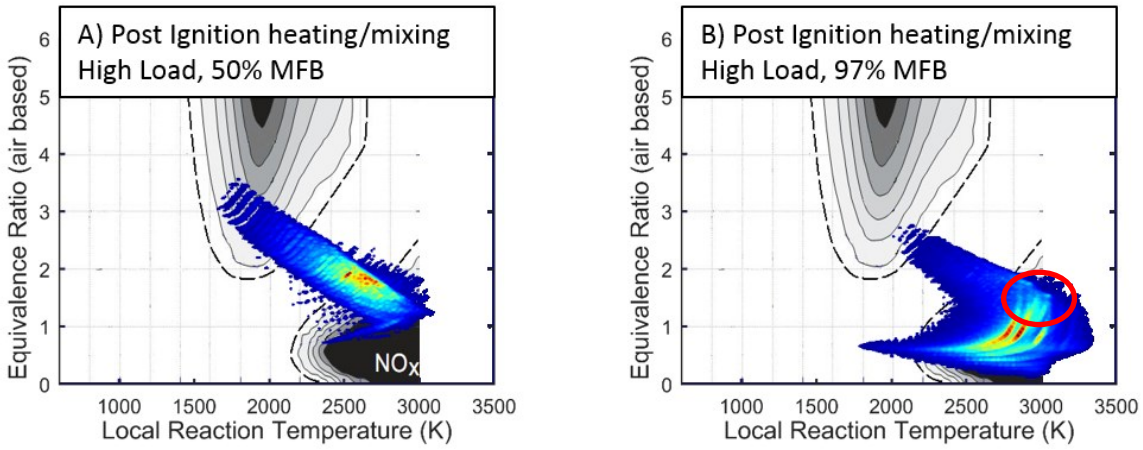

Figure 23 – Comparison of post ignition heating and mixing plots for 50% EGR rate, 816 bar injection pressure for both Conventional and LTC modes

SUMMARY AND CONCLUSIONS

A model to predict the combustion trajectories for a direct injection compression ignition engine was built using an existing spray model. This model uses the in-cylinder pressure and takes into account multiple different engine parameters at different operating conditions. The model is able to predict the equivalence ratio of small control volumes within the spray and the corresponding local flame temperature. The mass of fuel burned out of each control volume is then determined based on chemical kinetics and plotted on a Φ-T plot. When these plots are overlaid on soot and NOx formation region plots, a qualitative assessment of emissions can be conducted. This mode is presented to show its usefulness is describing the combustion behavior on different control strategies.

The plots presented show both the ignition location and the post-mixing heating and cooling trajectory in the spray throughout the complete combustion event. The plots illustrate how conventionally timed diesel injection can react at a high equivalence ratio and the bulk gas heating behavior will result in any soot that is formed to be oxidized. With the introduction of high EGR, the ignition locations move up into the soot zone due to less fresh air in the cylinder. The bulk gas does not heat as much, or cooling may even occur depending on the operating condition, indicating that the soot formed may not be oxidized. When late injection low temperature combustion is achieved with high EGR, both NO and soot formation can be controlled due to the delayed combustion phasing and increased mixing time. This may allow for some soot that is formed to heat and be oxidized. When the injection pressure in decreased for a specific operating condition, the ignition equivalence ratio increases, increasing the formation of

soot and decreasing the possible soot oxidation. When injection pressure is increase, the ignition equivalence ratio decreases, leading to higher temperatures and increased NOx formation.

At higher speeds and higher horsepower, the plots become less effective at determining the soot formation during the combustion process. This is possibly due the decrease in the total amount of oxygen in the cylinder.

The encouraging results obtained from this work suggest the proposed improved model can serve as a foundation for future development of control strategies.

REFERENCES

[1] Twigg, M. V., 2007, "Progress and future challenges in controlling automotive exhaust gas emissions," Applied Catalysis B: Environmental, 70(1), pp. 2-15.

[2] Kook, S., Bae, C., Miles, P. C., Choi, D., and Pickett, L. M., 2005, "The influence of charge dilution and injection timing on low-temperature diesel combustion and emissions," SAE Transactions - Journal of Fuels and Lubricants, 114(2005-01-3837), pp. 1575 - 1595.

[3] Gao, Z., and Schreiber, W., 2001, "A phenomenologically based computer model to predict soot and NOx emission in a direct injection diesel engine," International Journal of Engine Research, 2(3), pp. 177-188.

[4] Gao, Z., Conklin, J., Daw, C. S., and Chakravarthy, V. K., 2010, "A proposed methodology for estimating transient engine-out temperature and emissions from steady-state maps," International Journal of Engine Research, 11(2), pp. 137-151.

[5] Gao, Z., Wagner, R. M., Sluder, C., Daw, C. S., and Green, J., 2011, "Using a phenomenological computer model to investigate advanced combustion trajectories in a CIDI engine," Fuel, 90(5), pp. 1907-1918.

[6] Johri, R., Salvi, A., and Filipi, Z., 2012, "Real-time transient soot and NOx virtual sensors for diesel engine using neuro-fuzzy model tree and orthogonal least squares," Journal of Engineering for Gas Turbines and Power, 134(9), p. 092806.

[7] Glavmo, M., Spadafora, P., and Bosch, R., 1999, "Closed-loop start of combustion control utilizing ionization sensing in a diesel engine," SAE transactions, 108(3), pp. 799-807.

[8] Beasley, M., Cornwell, R., Fussey, P., King, R., Noble, A., Salamon, T., Truscott, A., and Landsmann, G., 2006, "Reducing diesel emissions dispersion by coordinated combustion feedback control," No. 0148-7191, SAE Technical Paper.

[9] Hasegawa, M., Shimasaki, Y., Yamaguchi, S., Kobayashi, M., Sakamoto, H., Kitayama, N., and Kanda, T., 2006, "Study on ignition timing control for diesel engines using in-cylinder pressure sensor," No. 0148-7191, SAE Technical Paper.

[10] Husted, H., Kruger, D., Fattic, G., Ripley, G., and Kelly, E., 2007, "Cylinder pressure-based control of pre-mixed diesel combustion," SAE paper(2007-01), p. 0773.

[11] Quillen, K. P., Viele, M., and Ciatti, S. A., "Next-cycle and same-cycle cylinder pressure based control of internal combustion engines," Proc. ASME 2010 Internal Combustion Engine Division Fall Technical Conference, American Society of Mechanical Engineers, pp. 635-645.

[12] Quillen, K. P., and Viele, M., "An analysis of next cycle control based on cylinder pressure derived calculations," Proc. ASME 2009 Internal Combustion Engine Division Fall Technical Conference, American Society of Mechanical Engineers, pp. 377-386.

[13] Bittle, J. A., and Jacobs, T. J., 2015, "A computationally efficient combustion trajectory prediction model developed for real-time diesel combustion control," International Journal of Engine Research, p. 1468087414566513.

[14] Musculus, M. P., and Kattke, K., 2009, "Entrainment waves in diesel jets," SAE International Journal of Engines, 2(1), pp. 1170-1193.

[15] Bittle, J. A., and Jacobs, T. J., "Combustion Trajectory Visualization Model for Study of Conventional and Advanced Direct Injection Combustion Modes," Proc. ASME 2015 Internal Combustion Engine Division Fall Technical Conference, American Society of Mechanical Engineers, pp. V001T003A004-V001T003A004.

[16] Pickett, L. M., Manin, J., Genzale, C. L., Siebers, D. L., Musculus, M. P., and Idicheria, C. A., 2011, "Relationship between diesel fuel spray vapor penetration/dispersion and local fuel mixture fraction," SAE International Journal of Engines, 4(1), pp. 764-799.

[17] Depcik, C., Jacobs, T., Hagena, J., and Assanis, D., 2007, "Instructional use of a single-zone, premixed charge, spark-ignition engine heat release simulation," International Journal of Mechanical Engineering Education, 35(1), p. 1.

[18] Brunt, M. F., and Platts, K. C., 1999, "Calculation of heat release in direct injection diesel engines," No. 0148-7191, SAE Technical Paper.

[19] Hohenberg, G. F., 1979, "Advanced approaches for heat transfer calculations," No. 0148-7191, SAE Technical paper.

[20] Bittle, J. A., and Jacobs, T. J., 2012, "On the relationship between fuel injection pressure and two-stage ignition behavior of low temperature diesel combustion," ASME Journal of Energy Resources Technology, 134(4), pp. 042201-042201 -- 042201-042206.

[21] Lancaster, D. R., Krieger, R. B., and Lienesch, J. H., 1975, "Measurement and analysis of engine pressure data," SAE Transactions, 84(SAE Paper No. 750026), pp. 155-172.

[22] Figliola, R., and Beasley, D., 2000, Theory and Design for Mechanical Measurements, John Wiley & Sons, Inc.